

Current Conservation in the Covariant Quark-Diquark Model of the Nucleon

M. Oettel¹, M. A. Pichowsky², and L. von Smekal³

¹ Universität Tübingen, Institut für Theoretische Physik, Auf der Morgenstelle 14, 72076 Tübingen, Germany

² Nuclear Theory Center, Indiana University, Bloomington IN 47405, USA, and
Department of Physics & Supercomputer Computations Research Institute, Florida State University,
Tallahassee, FL 32306-4130, USA

³ Universität Erlangen-Nürnberg, Institut für Theoretische Physik III, Staudtstr. 7, 91058 Erlangen, Germany

(30 September 1999)

Abstract. The description of baryons as fully relativistic bound states of quark and glue is possible so far only with neglecting irreducible 3-quark interactions and assuming separable 2-quark correlations. Under these circumstances the bound-state problem reduces to an effective Bethe-Salpeter equation in which the interaction kernel describes the quark-exchange necessary to implement the Pauli principle. The fully interacting 2-quark correlations include all the gluonic interactions of quarks in this picture. The separable 2-quark (diquark) correlators are employed to parameterize this less known part of the non-perturbative dynamics of quarks within baryons.

In the present article, an extension of the covariant quark-diquark model of baryons is introduced which allows for the inclusion of finite-sized, and thus more realistic quark substructure of the diquark correlations. An important consequence of this is that violations of the electromagnetic current conservation of the baryon occur in the impulse approximation which are no longer negligible. It is shown that current conservation is ensured only by the inclusion of contributions that arise from the nucleon Bethe-Salpeter kernel. In particular, these arise from the coupling of the photon to exchanged quark and direct “seagull” couplings to the diquark structure. These contributions are derived from the Ward and Ward-Takahashi identities. Current and charge conservation are proved to be manifest in this framework. Adopting a simple dynamical model of constituent quarks and exploring various parameterizations of scalar diquark correlations, the nucleon Bethe-Salpeter equation is solved, and from these solutions, charge conservation is verified in numerical calculations of the proton and neutron electromagnetic form factors. While the magnetic moments are still about 50% too small, the improvements necessary to remedy this are discussed, the results obtained in this framework are shown to provide an excellent description of the electric form factors (and charge radii) of the proton, up to a photon momentum transfer of 3.5GeV^2 , and the neutron.

PACS. 11.10.St (Bound states; Bethe-Salpeter equations) – 13.40.Gp (Electromagnetic form factors) – 14.20.Dh (Protons and neutrons)

1 Introduction

To the precision accessible to current measurements, the proton is the only known hadron that is stable under the effect of all interactions. Protons are thus ideal for use in beams or in targets for scattering experiments designed to explore the fundamental dynamics of the strong interaction. From this, it follows that more is known about the proton and its nearly stable isospin partner, the neutron, than any other hadrons. There is an abundance of observable properties of the nucleon, such as scattering properties, elastic scattering form factors, electromagnetic form factors and parton distributions, which are being measured with increasing precision at various accelerator facilities around the world. In particular, the ratio of the electric and the magnetic form factor of the proton is subject to current measurements at CEBAF, and recent results from MAMI [1] and NIKHEF [2] show that also the neutron is subject to current measurements with promising perspectives towards a precise knowledge of the electromagnetic properties of both nucleons. Hence, the development of an accurate and tractable covariant framework for the nucleon in terms of the underlying quarks and gluons is clearly desirable.

Models of the nucleon and other baryons are numerous and have had differing degrees of success in describing particular properties of baryons. Some of the frameworks that have been employed are non-relativistic [3, 4, 5] and relativistic [6] quark potential models, bag models [7, 8], skyrmion models [9, 10, 11, 12] or the chiral soliton of the Nambu-Jona-Lasinio (NJL) model [13, 14]. The relativistic bound state problem of 3-quark Faddeev type was studied extensively within the NJL model [15, 16, 17, 18, 19, 20] or its non-local generalization, the global color model [21, 22]. In addition, complementary aspects of some of these models are combined in, *e.g.*, the chiral bag model [23, 24] or also a hybrid model that implements the NJL-soliton picture of baryons within the quark-diquark Bethe-Salpeter (BS) framework [25].

The present study is concerned with the further development of a description of baryons (and the nucleon, in particular) as bound states of quarks and gluons in a fully-covariant quantum field theoretic framework based on the Dyson-Schwinger equations of QCD. Such a framework has already reached a high level of sophistication for mesons. In these studies, the quark-antiquark scattering kernel is modeled as a confined, non-perturbative gluon exchange. Such a gluon exchange can be provided by solutions to the Dyson-Schwinger equations for the propagators of QCD in the covariant gauge [26, 27]. In phenomenological studies the gross features of such solutions are mimicked by model assumptions on the quark-antiquark kernel. With this kernel, the dressed-quark propagator is obtained as the solution of its (quenched) Dyson-Schwinger equation (DSE), and the same kernel is then employed in the quark-antiquark Bethe-Salpeter equation (BSE) from which one obtains the meson bound states masses and BS amplitudes. Once the dressed-quark propagators and meson BS amplitudes have been obtained in this way, observables can then be calculated in a straight-forward man-

ner. The success of this approach has been demonstrated in many phenomenological applications of the framework, such as electromagnetic form factors [28], decay widths, π - π scattering [29], vector-meson electroproduction [30], and many others. Summaries of this Dyson-Schwinger/Bethe-Salpeter description of mesons may be found in Refs. [31, 32, 33].

The significantly more complicated framework required for an analogous description of baryons based on the quantum field theoretic description of bound states in 3-quark correlations has meant that baryons have received far less attention than mesons within this approach. Consequently, the utility of such a description for the baryons is considerably less understood, even on the phenomenological level. (For example, the ramifications of various truncation schemes, required in any quantum field theoretic treatment of bound states, which have been explored extensively in the meson sector are completely unknown in the baryon sector.) The developments in this direction employ a picture based on separable 2-quark correlations, *i.e.*, on diquarks, interacting with the 3rd quark in a manner which allows a relativistic bound state treatment much analogous to the BS problem [34, 35, 36]. Although each of these studies employs simplified model assumptions for the quark propagators and diquark correlators, they demonstrate the utility of the approach in general, and these simplified model assumptions can be replaced by more realistic ones in the future as more is understood about the underlying dynamics of quarks and gluons.

In the present article we generalize this framework for the 3-quark bound state problem in quantum field theory to accommodate quark-substructure within the separable diquark correlations. This necessary extension has important implications on the electromagnetic properties of the nucleons. We construct explicitly a conserved current for the electromagnetic couplings of the nucleons in this framework, and we prove charge conservation analytically. In particular, we employ Ward and Ward-Takahashi identities for the relevant quark correlations which arise from electromagnetic gauge invariance. In order to avoid unnecessary complications in the formal development, in our present study we employ simple constituent-quark and diquark propagators. However, the generalization to include dressed propagators, in particular, to account for confined quark and diquark correlations, is discussed and requires minor modifications.

The organization of the article is as follows. In Sec. 2, the properties of the two-quark correlations (or diquarks), used herein, are introduced and discussed and the important role of constructing a diquark correlator that is antisymmetric under quark exchange is emphasized. For the purposes of the present study, only Lorentz-scalar, isoscalar diquarks are considered. Of course, diquark correlations other than the scalar diquark may be necessary for a complete picture of the nucleon. Certainly, the inclusion of other channels, such as the axialvector diquark, is necessary for a description of the octet and decuplet baryons. Nonetheless, for the purposes of the present study, only scalar diquarks are considered; the generaliza-

tion to include other diquarks is straight-forward [36]. In Sec. 3, the nucleon BS equation and the quark-exchange kernel are introduced and solved numerically, and the independence of solutions on the momentum partitioning parameter η is assessed. In Sec. 4, the normalization condition for the nucleon BS amplitude is derived and the nucleon electromagnetic current is obtained in Sec. 5. In Sec. 5.1, the “seagull” contributions to the electromagnetic current, necessary for current conservation, are derived from the Ward and Ward-Takahashi identities. In Sec. 6, expressions for the electromagnetic form factors of the nucleon are derived, the numerical calculations are described in Sec. 6.1, and the results for the form factors are presented and discussed in Sec. 6.2. Conclusions from this study are provided in Sec. 7. Several appendices have also been included. These provide details of the framework, which although rather involved, may provide additional insights for the interested reader.

2 Diquark Correlations

Although non-relativistic 3-body Faddeev equations can be exactly solved within a given potential model, the analogous problem in quantum field theory requires truncation of the interaction kernel before a solution may be obtained. A widely-employed truncation scheme is to neglect contributions to the Faddeev kernel which arise from irreducible 3-quark interactions. This allows one to rewrite the Dyson series for the 3-quark Green function as a nested system of coupled equations, one being the BS equation for the 2-quark T -matrix and the other, the Faddeev equation, which describes the coupling of the 3rd quark to these 2-quark correlations. As a result, the nature of the gluonic interactions of quarks enters only in the BSE of the 2-quark subsystem, *i.e.*, in the quark-quark interaction kernel. The full inhomogeneous BS problem for this 2-quark system is avoided by assuming separable contributions (to be explained below), hereafter referred to as diquarks, to account for the relevant 2-quark correlations within the hadronic bound state.

While in the NJL model the 2-quark T -matrix has the property of being separable, in general this additional assumption is at present necessary to simplify the 3-quark bound state problem in quantum field theory. Such separable contributions could, *e.g.*, arise as (finite sum of) isolated poles at timelike values P^2 of the 2-quark total momentum P describing diquark bound states. Such poles allow the use of homogeneous BSEs to obtain the respective amplitudes from the gluonic interaction kernel of the quarks, and thus to calculate these separable contributions to the 2-quark T -matrix in this way.

However, the validity of using a diquark correlator to parameterize the 2-quark correlations phenomenologically, does not rely on the existence of asymptotic diquark states. Rather, the diquark correlator may be devoid of singularities for timelike momenta, which may be interpreted as one possible realization of diquark confinement. In principle, one may appeal to models employing a general, separable diquark correlator which need not have

any simple analytic structure, in which case no particle interpretation for the diquark would be possible.

Herein, a “diquark correlation” thus refers to the use of a separable 4-quark function in the $\bar{3}$ channel of the $SU(3)$ color group. The utility of such diquark correlations for a description of baryon bound states is a central element of the present approach, it serves to simplify the necessary formalism. To provide a simple demonstration of the general framework, and its application to the calculation of nucleon form factors, we assume that the diquark correlator corresponds to one simple scalar-diquark pole at $P^2 = m_s^2$ which is both separable and constituent-like. In this simplest description within the present approach the (color-singlet) baryon thus is a bound state of a color-3 quark and a color- $\bar{3}$ (scalar) diquark correlation. It should be emphasized that the use of diquark correlations in this capacity is quite general and does not necessarily imply the existence of asymptotically-free diquark states, which have not been observed experimentally. The generalization to separable but confined two-quark correlations is straight-forward and does not introduce significant changes to the framework.

The absence of asymptotic-diquark states may be explained in a number of ways. Although, it has been observed that solutions of the BSE in ladder approximation yield asymptotic color- $\bar{3}$ diquark states [37], when terms beyond the ladder approximation are maintained, the diquarks cease to be bound [38]. That is, the addition of terms beyond the ladder approximation to the BS kernel, in a way which preserves Goldstone’s theorem at every order, has a minimal impact on solutions for the color-singlet meson channels. In contrast, such terms have a significant impact on the color- $\bar{3}$ diquark channels. In Ref. [38], it was demonstrated that these contributions to BS kernel beyond ladder approximation are predominantly repulsive in the color- $\bar{3}$ diquark channel. It was furthermore demonstrated in a simple confining quark model that the strength of these repulsive contributions suffices to move the diquark poles from the timelike P^2 -axis and far into the complex P^2 -plane. While the particular, confining quark model is in conflict with locality, the same effect was later verified within the NJL model [39]. This suggests that this mechanism for diquark confinement, to eliminate the possibility of ever producing asymptotic diquark states, might hold independent of the particular realization of quark confinement.

In a local quantum field theory description, on the other hand, colored asymptotic states do exist, for the elementary fields as well as for possible colored composites such as the diquark, but not in the physical subspace of the indefinite metric space of covariant gauge theories. The analytic structure of correlation functions, the holomorphic envelope of extended permuted tubes in coordinate space, is much the same in this description as in quantum field theory with a positive definite inner product (Hilbert) space. In particular, 2-point correlations in momentum space are generally analytic functions in the cut complex P^2 -plane with the cut along the timelike real axis. Confinement is interpreted as the observation that both

$$G_{\alpha\beta\gamma\delta}^{\text{sep}}$$

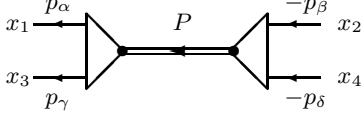


Fig. 2.1. The diquark pole in the 4-quark Green's function.

absorptive as well as anomalous thresholds in hadronic amplitudes are due only to other hadronic states [40]. The phenomenological implementation of this algebraic notion of confinement seems much harder to realize, however.

For the present purposes of developing a general framework for the description of baryon bound states, the question as to whether one should or should not model the diquark correlations in terms of functions with or without singularities for total timelike momentum P^2 is irrelevant. We reiterate, however, that the framework in principle suits to accommodate both of these descriptions of confinement by straight-forward modifications.

The goal of the present study is simply to assess the utility of describing baryons as bound states of quark and diquark correlations, in a framework in which the diquark correlations are assumed to be *separable*. (The term separable refers to the property that a 4-point Green function $G(p, q; P)$ be independent of the scalar qp , where q and p are the relative momenta of the two incoming and outgoing particles, respectively, and P is the total momentum.) To this end, we employ constituent-quark and constituent-diquark propagators (which have simple poles for timelike momenta P^2).

Assuming identical quarks, consider the 4-point quark Green function in coordinate space given by

$$G_{\alpha\beta\gamma\delta}(x_1, x_2, x_3, x_4) = \langle T(q_\gamma(x_3)q_\alpha(x_1)\bar{q}_\beta(x_2)\bar{q}_\delta(x_4)) \rangle, \quad (2.1)$$

where α, β, γ , and δ denote the Dirac indices of the quarks and T denotes time-ordering of the quark fields $q_\alpha(x)$. The assumption of a separable diquark correlator, corresponding to the diagram shown in Fig. 2, can be written in momentum space as $G_{\alpha\beta\gamma\delta}^{\text{sep}}(p, q, P)$ where

$$G_{\alpha\beta\gamma\delta}^{\text{sep}}(p, q, P) := e^{-iPY} \int d^4X d^4y d^4z e^{iqz} e^{-ipy} e^{iPX} G_{\alpha\beta\gamma\delta}^{\text{sep}}(x_1, x_2, x_3, x_4) = D(P) \chi_{\gamma\alpha}(p, P) \bar{\chi}_{\beta\delta}(q, P), \quad (2.2)$$

where $D(P)$ is the diquark propagator, $X = \sigma x_1 + (1 - \sigma)x_3$, $Y = (1 - \sigma')x_2 + \sigma'x_4$, the total momentum partitioning of the outgoing and incoming quark pairs are given respectively by σ and σ' both in $[0, 1]$, and $y = x_1 - x_3$, $z = x_2 - x_4$.

As described above, the separable form of the diquark correlation of Eq. (2.2) does not necessarily entail the existence of an asymptotic diquark state. The framework developed herein makes no restrictions on the particular choice of the diquark propagator $D(P)$. Technically in

fact, model correlations which mimic confinement through the absence of timelike poles are easy to implement as shown in Ref. [35].

Nonetheless, for the purpose of demonstration, here we employ the simplest form for this propagator corresponding to a simple (scalar) diquark bound state in the 2-quark Green function G of Eq. (2.1). The appearance of such an asymptotic diquark state requires the diquark propagator have a simple pole at $P^2 = m_s^2$, where m_s is the mass of the diquark bound state, *i.e.*,

$$D(P) = \frac{i}{P^2 - m_s^2 + i\epsilon}. \quad (2.3)$$

Then $\chi(p, P)$ and its adjoint $\bar{\chi}(p, P) = \gamma_0 \chi^\dagger(p, P) \gamma_0$ are the BS wave functions of the (scalar) diquark bound state which are defined as the matrix elements of two quark fields or two antiquark fields between the bound state and the vacuum, respectively. Further details concerning these definitions are given in Appendix A.

It is convenient to define the *truncated* diquark BS amplitudes (sometimes referred to as BS vertex functions) $\tilde{\chi}$ and $\tilde{\bar{\chi}}$ from the BS wave functions in Eq. (2.2) by amputating the external quark propagators,

$$\tilde{\chi}(p, P) := S^{-1}((1 - \sigma)P + p) \chi(p, P) S^{-1T}(\sigma P - p), \quad (2.4)$$

$$\tilde{\bar{\chi}}(p, P) := S^{-1T}(\sigma P - p) \bar{\chi}(p, P) S^{-1}((1 - \sigma)P + p). \quad (2.5)$$

The convention employed here is to use the same symbols for both the BS wave functions and the truncated BS amplitudes, with the latter denoted by a tilde. An important observation made in Appendix A, which is of use in the following discussions, is that the for identical quarks, antisymmetry under quark exchange constrains the diquark BS amplitudes $\tilde{\chi}$ to satisfy:

$$\tilde{\chi}(p, P) = -\tilde{\chi}^T(-p, P)|_{\sigma \leftrightarrow (1 - \sigma)}. \quad (2.6)$$

Note that σ and $(1 - \sigma)$ have been interchanged here.

In principle, at this point one could go ahead and specify the form of the kernel for the quark-quark BSE in ladder approximation, and obtain diquark BS amplitudes in much the same manner in which solutions for the mesons are obtained. However, as discussed above, the appearance of stable bound state solutions might be an artifact of the ladder approximation rather than the true nature of the quark-quark scattering amplitude. Therefore, for our present purposes various simple model parameterizations for diquark BS amplitudes are explored, rather than employing a particular solution of the diquark homogeneous BSE. The motivation behind the employment of such parametrized amplitudes is to explore the general aspects and implications of using a separable diquark correlation for the description of the nucleon bound state.

For separable contributions of the pole type (2.3), but possibly complex mass (with $\text{Re}(m_s^2) > 0$), one readily obtains standard BS normalization conditions to fix the overall strength of the quark-quark coupling to the diquark for a given parameterization of the diquark structure. These are obtained from the inhomogeneous quark-quark BSE

for the Green function of Eq. (2.1) employing pole dominance for P^2 sufficiently close to m_s^2 .¹ To sketch their derivation consider the inhomogeneous BSE which is of the general form,

$$G(p, q, P) = \left(G^{(0)-1}(p, q, P) - K(p, q, P) \right)^{-1}. \quad (2.7)$$

Here $G^{(0)}$ denotes the antisymmetric Green function for the disconnected propagation of two identical quarks. The definition of its inverse $G^{(0)-1}$ and a brief discussion of how to derive it, may be found in Appendix A. With the simplifying assumption that the quark-quark interaction kernel K be independent on the total diquark momentum P ; that is, $K(p, q, P) \equiv K(p, q)$ (which is satisfied in the ladder approximation for example), the derivative of G with respect to the total momentum P , gives the relation

$$-P^\mu \frac{\partial}{\partial P^\mu} G(p, q, P) = \int \frac{d^4 k}{(2\pi)^4} \frac{d^4 k'}{(2\pi)^4} \quad (2.8)$$

$$G(p, k, P) \left(P^\mu \frac{\partial}{\partial P^\mu} G^{(0)-1}(k, k', P) \right) G(k', q, P).$$

Upon substitution of $G(p, q, P)$ as given by Eqs. (2.2) and (2.3), and equating the residues of the most singular terms, one obtains the non-linear constraint for the normalization of the diquark BS amplitudes χ and $\tilde{\chi}$,

$$1 \stackrel{!}{=} \frac{-i}{4m_s^2} \int \frac{d^4 p}{(2\pi)^4} \quad (2.9)$$

$$\left\{ \text{tr} \left(S^T(p_\beta) \tilde{\chi}(p, P) \left(P \frac{\partial}{\partial P} S(p_\alpha) \right) \tilde{\chi}(p, P) \right) \right.$$

$$\left. + \text{tr} \left(\tilde{\chi}(p, P) S(p_\alpha) \tilde{\chi}(p, P) \left(P \frac{\partial}{\partial P} S^T(p_\beta) \right) \right) \right\},$$

where $p_\alpha = p + (1-\sigma)P$ and $p_\beta = -p + \sigma P$, *i.e.*, $P = p_\alpha + p_\beta$ and $p = \sigma p_\alpha - (1-\sigma)p_\beta$. The scalar diquark contribution, relevant to the present study of the nucleon bound state, is color- $\bar{3}$ and isosinglet. Lorentz covariance requires its Dirac structure to be the sum of four independent contributions, each proportional to a function of two independent momenta. For simplicity only a single term is maintained here, which has the following structure:

$$\tilde{\chi}(p, P) = \gamma_5 C \frac{1}{N_s} \tilde{P}(p^2, pP), \quad (2.10)$$

where C is the charge conjugation matrix ($C = i\gamma_2\gamma_0$ in the standard representation). The normalization constant N_s is fixed from the condition given in Eq. (2.9) for a given form of $\tilde{P}(p^2, pP)$.

It may seem reasonable to neglect the dependence of this invariant function on the scalar pP ; such a simplification would yield the leading moment of an expansion of the angular dependence in terms of orthogonal polynomials, which has been shown to provide the dominant contribution to the meson bound state amplitudes in many

¹ For other separable contributions, *e.g.*, of the form of non-trivial entire functions for which one necessarily has a singularity at $|P^2| \rightarrow \infty$, the use of the inhomogeneous BSE to derive normalization conditions relies on the existence of full solutions to (2.7) of the separable type.

circumstances. However, in the present case the antisymmetry of the diquark wave function, *c.f.*, Eqs. (2.6), entails that

$$\tilde{P}(p^2, pP) = \tilde{P}(p^2, -pP) \Big|_{\sigma \leftrightarrow (1-\sigma)}. \quad (2.11)$$

For $\sigma \neq 1/2$ and thus for $\bar{p} := p|_{\sigma \leftrightarrow (1-\sigma)} \neq p$, it is thus not possible to neglect the pP dependence in the amplitude without violating the quark-exchange antisymmetry. To maintain the correct quark-exchange antisymmetry, we assume instead that the amplitude depends on both scalars, p^2 and pP in a specific way. In particular, we assume the diquark BS amplitude is given by a function that depends on the scalar

$$x := p_\alpha p_\beta - \sigma(1-\sigma)m_s^2 = -(1-2\sigma)pP - p^2$$

$$= (1-2\sigma)\bar{p}P - \bar{p}^2 \quad (2.12)$$

with $\bar{p} = (1-\sigma)p_\alpha - \sigma p_\beta$ and $p_{\{\alpha, \beta\}}$ as given above. For equal momentum partitioning between the quarks in the diquark correlation $\sigma = 1/2$, the scalar x reduces to the negative square of the relative momentum, $x = -p^2$. The two scalars that may be constructed from the available momenta p and P (noting that $P^2 = m_s^2$ is fixed) which have definite symmetries under quark exchange are given by the two independent combinations $p_\alpha p_\beta$ (which is essentially the same as above x) and $p_\alpha^2 - p_\beta^2$. The latter may only appear in odd powers which are associated with higher moments of the BS amplitude. Hence, these are neglected by setting

$$\tilde{P}(p^2, pP) \equiv P(x) \quad (2.13)$$

which can be shown to satisfy the antisymmetry constraint given by Eq. (2.11) $\forall \sigma \in [0, 1]$. Finally, the diquark BS normalization N_s , as obtained from Eq. (2.9), is given by

$$N_s^2 = \frac{-i}{4m_s^2} \int \frac{d^4 p}{(2\pi)^4} P^2(x)$$

$$P \frac{\partial}{\partial P} \text{tr} [S(p + (1-\sigma)P) S(-p + \sigma P)]. \quad (2.14)$$

The numerical results presented in the following sections explore the ramifications of several Ansätze for $P(x)$,

$$P_{n-P}(x) = \left(\frac{\gamma_n}{x + \gamma_n} \right)^n \text{ or } P_{\text{EXP}}(x) = \exp \{-x/\gamma_{\text{EXP}}\}, \quad (2.15)$$

where the integer $n = 1, 2, \dots$ and corresponds to monopole, dipole, ... diquark BS amplitudes. Their widths $\gamma_n, \gamma_{\text{EXP}}$ are determined from the nucleon BSE by varying them until the diquark normalization given by Eq. (2.14) and coupling strength g_s^2 necessary to produce the correct nucleon bound-state mass are equal. This is carried out numerically and described in detail in Sec. 3.

For completeness, various Gaussian forms that peak for values of $x = x_0 \geq 0$,

$$P_{\text{GAU}}(x) = \exp \{-(x - x_0)^2/\gamma_{\text{GAU}}^2\}, \quad (2.16)$$

are also explored. Such forms with finite x_0 were suggested for diquark amplitudes as a result of a variational calculation of an approximate diquark BSE in Ref. [41] and have been used in the nucleon calculations of Ref. [22].

Therein, a fit to the Gaussian form given by Ref. [41] (and Eq. (2.16) above) was employed with a width of $\gamma_{\text{GAU}} \simeq 0.11 \text{GeV}^2$ and $x_0/\gamma_{\text{GAU}} \simeq 1.7$. From a calculation within the present framework, which is described in Sec. 3, we observe that the necessary value for γ_{GAU} to obtain a reasonable nucleon mass is about an order of magnitude smaller than the value given in Ref. [22]. Furthermore in Sec. 6, we observe that the effect of a finite x_0 on the electric form factor of the neutron rules out the use of a Gaussian form with $x_0 \neq 0$ phenomenologically.

Some of the parameterizations used for diquark correlations in previous quark-diquark model studies of the nucleon [34, 35, 36], correspond to neglecting the substructure of diquarks entirely; this may be reproduced in the present framework by setting $\hat{P}(p^2, pP) = 1$. By neglecting the diquark substructure, the diquark BS normalizations such as N_s here are not well-defined, however. The strengths of the quark-diquark couplings are undetermined and chosen as free adjustable parameters of the model (one for each diquark channel maintained). In the present, more general approach, these couplings are determined by the normalizations of the respective diquark amplitudes. At present this is the scalar diquark normalization N_s alone which in turn determines the coupling strength $g_s = 1/N_s$ between the quark and diquark which binds the nucleon.

The aim of our present study is to generalize the notion of diquark correlations by going beyond the use of a point-like diquark and include a diquark substructure in a form similar to that of mesons. In the most general calculation of the three-body bound state, the strength of the quark-diquark coupling is not at one's disposal; it arises from the elementary interactions between the quarks. By using the diquark BS normalization condition of Eq. (2.14), we can assess whether the quark-diquark picture of the nucleon is still able to provide a reasonable description of the nucleon bound state if the coupling strength is obtained from the diquark BSE rather than forcing the quark and diquark to bind by adjusting their couplings freely.

In this approach, the question as to whether the quark-diquark coupling is sufficiently strong to produce bound baryons will eventually be determined by the strength of the model quark-quark interaction kernel that leads to the diquark BS amplitude.

Finally, the use of a diquark BS amplitude with a *finite* width improves on the previous calculations in yet another respect. Without the substructure of the diquark, an additional ultraviolet regularization had to be introduced in the exchange kernel of the BSE for the nucleon in Refs. [34, 35, 36]. In the present study, the finite-sized substructure of the diquark leads to a nucleon BSE which is completely regular in the ultraviolet in a natural way.

In this section, we have discussed some general features of the diquark amplitude employed in our present study. The important observations are the implications of its antisymmetry under quark exchange which constrains the functional dependence on the quark momenta, and the derivation of the BS normalization condition, Eq. (2.14), to fix the quark-diquark coupling strength. By taking these into account, we will find that the precise form of the

Ansatz for the diquark BS amplitude $P(x)$ has little qualitative influence on the resulting nucleon amplitudes as long as $P(x)$ falls off by at least one power of x for large x corresponding to a large spacelike relative momentum.

3 The Quark-Diquark Bethe-Salpeter Equation of the Nucleon

By neglecting irreducible 3-quark interactions in the kernel of the Faddeev equation giving the 6-point Green function that describes the fully-interacting propagation of 3 quarks, the Dyson series for this 6-point Green function reduces to a coupled set of two-body Bethe-Salpeter equations, see, *e.g.*, Ref. [18]. As discussed in the previous section, for the purpose of demonstrating the framework developed herein, we choose to employ constituent quark and diquark propagators. However, the framework itself is much more general. The assumptions under which it is developed require only that the irreducible 3-quark interactions are neglected in the nucleon Faddeev kernel and that the diquark correlations be well-parametrized by a sum of separable terms (which may or may not have poles associated with asymptotic diquark states).

Maintaining only the (flavor-singlet, color- $\bar{3}$) scalar diquark channel in these correlations, corresponding to Eqs. (2.2) and (2.3), the appearance of a stable nucleon bound state coincides with the development of a pole in the Green function $G_{\alpha\beta}$ describing the fully-interacting (spin-1/2) quark and (scalar) diquark correlations which is of the form,

$$G_{\alpha\beta}^{\text{pole}}(p, k, P_n) = \left(\psi(p, P_n) \frac{i(\not{P}_n + M_n)}{P_n^2 - M_n^2 + i\epsilon} \bar{\psi}(-k, P_n) \right)_{\alpha\beta}. \quad (3.1)$$

Here k and p are the relative momenta between the quark and diquark, incoming and outgoing, respectively, P_n is the four-momentum of the nucleon with mass M_n , α and β denote the Dirac indices of the quark, and the nucleon BS wave function $\psi(p, P_n)$ is related to its adjoint according to

$$\bar{\psi}(p, P_n) = \gamma_0 \psi^\dagger(-p, P_n) \gamma_0 = C \psi^T(p, -P_n) C^{-1}. \quad (3.2)$$

The truncated nucleon BS amplitude $\tilde{\psi}$ is defined as

$$\psi(p, P_n) = D((1-\eta)P_n - p) S(\eta P_n + p) \tilde{\psi}(p, P_n), \quad (3.3)$$

where $\eta \in [0, 1]$ is the fraction of the nucleon momentum P_n carried by the quark. The resulting homogeneous Bethe-Salpeter equation for the nucleon bound state reads,

$$\tilde{\psi}_{\alpha\beta}(p, P_n) = \int \frac{d^4k}{(2\pi)^4} K_{\alpha\gamma}(p, k; P_n) \psi_{\gamma\beta}(k, P_n), \quad (3.4)$$

where $K_{\alpha\beta}(p, k; P_n)$ is the kernel of the nucleon BSE which represents the exchange of one of the quarks within the diquark with the spectator quark. Maintaining the quark-exchange antisymmetry of the diquark correlations, this kernel provides the full antisymmetry within the nucleon

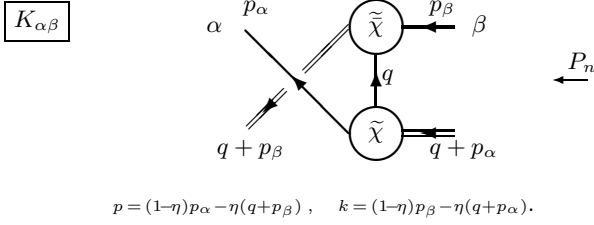


Fig. 3.1. The quark-exchange kernel of the nucleon BSE.

(i.e., Pauli's principle) in the quark-diquark model [15]. The exchange kernel is shown in Fig. 3 and given by

$$K_{\alpha\beta}(p, k; P_n) = \quad (3.5)$$

$$-\frac{1}{2} \tilde{\chi}_{\alpha\gamma}(p_1, q + p_\alpha) S_{\gamma\delta}^T(q) \tilde{\chi}_{\delta\beta}^T(p_2, q + p_\beta) \\ = \frac{1}{2N_s^2} P(x_1)P(x_2) S_{\alpha\beta}(q), \quad (3.6)$$

where the factor $-1/2$ arises from the flavor coupling between the quark and diquark and p_1 and p_2 are the relative momenta of the quarks within the incoming and outgoing diquark, respectively, such that

$$p_1 = \sigma p_\alpha - (1-\sigma)q, \quad \text{and} \quad p_2 = (1-\sigma')q - \sigma' p_\beta. \quad (3.7)$$

The respective momentum partitionings are σ and σ' and need not be equal. The total momenta of the incoming and the outgoing diquark are $q+p_\alpha$ and $q+p_\beta$. The momentum q of the exchanged quark is expressed in terms of the total nucleon momentum P_n and relative momenta k and p as

$$q = (1-2\eta)P_n - p - k. \quad (3.8)$$

Using the definitions of q and the quark momenta $p_\alpha = \eta P_n + p$ and $p_\beta = \eta P_n + k$, the relative momenta in the diquark BS amplitudes can be expressed as

$$p_1 = (\sigma\eta - (1-\sigma)(1-2\eta))P_n + (1-\sigma)k + p, \quad (3.9)$$

$$p_2 = ((1-\sigma')(1-2\eta) - \sigma'\eta)P_n - k - (1-\sigma')p. \quad (3.10)$$

The corresponding arguments of the quark-exchange-antisymmetric diquark BS amplitudes follow readily from their definition in Eq. (2.12),

$$x_1 = -p_1^2 - (1-2\sigma)((1-\eta)p_1 P_n - p_1 k), \quad (3.11)$$

$$x_2 = -p_2^2 + (1-2\sigma')((1-\eta)p_2 P_n - p_2 p). \quad (3.12)$$

Before proceeding, it is worth summarizing some of the important aspects of this framework:

1. The dependence of the exchange kernel on the total nucleon bound-state momentum P_n is *crucial* in order to obtain the correct relationship between the electromagnetic charges of the proton and neutron bound states and the normalizations of their BS amplitudes.
2. The momentum q of the exchanged quark is *independent* of the nucleon momentum P_n *only* for the particular value of momentum partitioning $\eta = 1/2$.

3. The relative momenta p_1 and p_2 of the quarks within the diquarks are only independent of the total momentum P_n of the nucleon for the particular choice:

$$\sigma = \sigma' = \frac{1-2\eta}{1-\eta}. \quad (3.13)$$

The *symmetric* arguments of x_1 and x_2 in the diquark BS amplitudes are independent of the total momentum P_n only if, in addition to the above criteria, $\sigma = \sigma' = 1/2$ as well, and hence $\eta = 1/3$. In fact, this conclusion can be further generalized: Any exchange-symmetric argument of the diquark amplitude can differ from the definition of Eq. (2.12) only by a term that is proportional to the square of the total diquark momentum. From this, it is possible to show that the diquark BS amplitudes can be independent of P_n only if $\eta = 1/3$. This is shown in Appendix B.

Unlike the ladder-approximate kernels commonly employed in phenomenological studies of the meson BSE, the quark-exchange kernels of the BSEs for baryon bound states, such as the present one depicted in Fig. 3, *necessarily* depend on the total momentum of the baryon P_n for *all* values of $\eta \in [0, 1]$. This has important implications on the normalization of the bound-state BS amplitudes as well as on the calculation of the electromagnetic charges of the bound states. In particular, considerable extensions of the framework beyond the impulse approximation are required in the calculation of electromagnetic form factors in order to ensure that the electromagnetic current is conserved for baryons. This issue is explored in detail in Sec. 5.

The form of the pole contribution arising from the nucleon bound state to the quark-diquark 4-point correlation function in Eq. (3.1) constrains the nucleon BS amplitude to obey the identities:

$$\tilde{\psi}(p, P_n)\Lambda^+(P_n) = \tilde{\psi}(p, P_n), \quad (3.14)$$

$$\Lambda^+(P_n)\tilde{\psi}(p, P_n) = \tilde{\psi}(p, P_n), \quad (3.15)$$

where $\Lambda^+(P_n) = (\not{P}_n + M_n)/2M_n$. It follows from this that the most general Lorentz-covariant form of the nucleon BS amplitude can be parameterized by

$$\tilde{\psi}(p, P_n) = \quad (3.16)$$

$$S_1(p, P_n)\Lambda^+(P_n) + S_2(p, P_n)\Xi(p, P_n)\Lambda^+(P_n),$$

$$\tilde{\psi}(p, P_n) = \quad (3.17)$$

$$S_1(-p, P_n)\Lambda^+(P_n) + S_2(-p, P_n)\Lambda^+(P_n)\Xi(-p, P_n),$$

where $\Xi(p, P_n) = (\not{p} - pP_n/M_n)/M_n$, and $S_1(p, P_n)$ and $S_2(p, P_n)$ are Lorentz-invariant functions of p and P_n . This provides a separation of the positive and negative energy components of the nucleon BS amplitude. In Appendix B, some of the consequences of this decomposition are explored. In particular, it allows one to rewrite the homogeneous BSE of Eq. (3.4) in a compact manner, in terms of a 2-vector $S^T(p, P_n) := (S_1(p, P_n), S_2(p, P_n))$ as

$$S(p, P_n) = \quad (3.18)$$

$$\frac{1}{2N_s^2} \int \frac{d^4k}{(2\pi)^4} P(x_1)P(x_2) D(k_s) T(p, k, P_n) S(k, P_n),$$

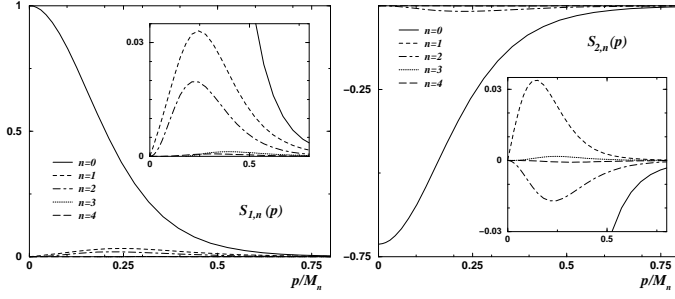


Fig. 3.2. The first 5 moments of the nucleon BS amplitudes S_1 (left) and S_2 (right).

where $k_s = (1-\eta)P_n - k$ and $T(p, k, P_n)$ is a 2×2 matrix in which each of the four elements is given by a trace over the Dirac indices of the quark propagator $S(k_q)$ (with $k_q = \eta P_n + k$), the propagator $S(q)$ of the exchanged quark and a particular combination of Dirac structures derived from the decomposition of the nucleon amplitude in Eq. (3.16), see Appendix B.

Upon carrying out these traces, the resulting BSE is transformed into the Euclidean metric by introducing 4-dimensional polar coordinates corresponding to the rest frame of the nucleon according to the following prescriptions (where “ \rightarrow ” denotes the formal transition from the Minkowski to the Euclidean metric):

$$p^2 \rightarrow -p^2, \quad P_n^2 \rightarrow M_n^2, \quad pP_n \rightarrow iM_n p y, \quad (3.19)$$

and $S(p, P_n) \rightarrow S(p, y)$.

Written in terms of these variables, the nucleon BS amplitude is a function of the square of the relative momentum p^2 and the cosine $y \in [-1, +1]$ of the azimuthal angle between the four-vectors p and P_n . The dependence of the nucleon BS amplitudes $S(p, y)$ on the angular variable y is approximated by an expansion to the order N in terms of the complete set of Chebyshev polynomials $T_n(y)$,

$$S(p, y) \simeq \sum_{n=0}^{N-1} (-i)^n S_n(p) T_n(y) \quad (3.20)$$

$$S_n(p) = i^n \frac{2}{N} \sum_{k=1}^N S(p, y_k) T_n(y_k), \quad (3.21)$$

$$\text{where } y_k = \cos\left(\frac{\pi(k-1/2)}{N}\right)$$

are the zeros of the Chebyshev polynomial $T_N(y)$ of degree N in y . Here, we employ Chebyshev polynomials of the first kind with a convenient (albeit non-standard) normalization for the zeroth Chebyshev moment from setting $T_0 = 1/\sqrt{2}$. The explicit factor of $(-i)^n$ is introduced into Eq. (3.20) to ensure that the moments $S_n(p)$ are real functions of positive $p \equiv \sqrt{p^2}$ for all n . The BSE for these moments of the nucleon BS amplitude is then

$$S_m(p) = -\frac{1}{2N_s^2} \int \frac{k^3 dk}{(4\pi)^2} \sum_{n=0}^{N-1} i^{m-n} T_{mn}(p, k) S_n(k), \quad (3.22)$$

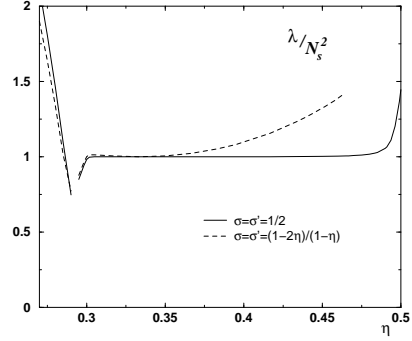


Fig. 3.3. Dependence of λ/N_s^2 on η for fixed $\sigma = \sigma' = 1/2$ (solid) and with σ, σ' from Eq. (3.13) (dashed). The width γ_2 is fixed to yield $\lambda/N_s^2 = 1$ at $\eta = 1/3$.

where the $(2N \times 2N)$ matrix $T_{mn}(p, k)$ is obtained from $T(p, k, P_n)$ by expanding in terms of Chebyshev polynomials both amplitudes S in the nucleon BSE of Eq. (3.18); that is, summing over the y_k on both sides of Eq. (3.18) according to Eq. (3.21) and using Eq. (3.20) for the BS amplitude on the right-hand side. The definition of the matrix T_{mn} appearing in Eq. (3.22) furthermore includes the explicit diquark propagator and BS amplitudes $P(x_1)$ and $P(x_2)$ of the integrand in Eq. (3.18) as well as the integrations over all angular variables. Its exact form is provided in Appendix B.

In the calculations presented herein, we restrict ourselves to the use of free propagators for constituent quark and diquark, with masses m_q and m_s respectively, as the simplest model to parameterize the quark and diquark correlations within the nucleon. Measuring all momenta in units of the nucleon bound-state mass M_n leaves m_q/M_n and m_s/M_n as the only free parameters at the present stage of the model. Using for the scalar diquark amplitude $P(x)$ the forms of Eqs. (2.15) or (2.16) with fixed widths γ , the homogeneous BSE for the nucleon in Eq. (3.4) is converted into an eigenvalue equation of the form,

$$\lambda \tilde{\psi}(p, P_n) = \int \frac{d^4 k}{(2\pi)^4} N_s^2 K(p, k, P_n) \psi(p, P_n), \quad (3.23)$$

with the additional constraint that $\lambda = N_s^2$ (note that $N_s^2 K$ is independent of N_s). This equation is solved iteratively and the largest eigenvalue λ is found which corresponds to the nucleon ground-state. To implement the constraint, we calculate the diquark normalization N_s^2 from Eq. (2.14) and compare it to the eigenvalue λ . This procedure is repeated with a new value for the width γ of the diquark BS amplitude until the eigenvalue obtained from the BSE agrees with the normalization integral in Eq. (2.14); that is, until the constraint $\lambda = N_s^2$ is satisfied.

A typical solution of the nucleon BSE is shown in Fig. 3.2. Five orders were retained in the Chebyshev expansion. The figure depicts the relative importance of the first four Chebyshev moments of the nucleon amplitudes $S_1(p, P_n)$ and $S_2(p, P_n)$. The respective results for their fifth moments are too small ($\leq 10^{-4}$) to be distinguished from zero on the scale of Fig. 3.2. This provides an indica-

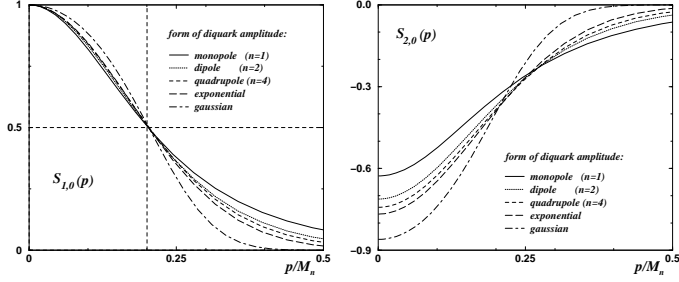


Fig. 3.4. The leading moments of the nucleon BS amplitudes S_1 (left) and S_2 (right) for the diquark amplitudes (2.15,2.16) with m_q adjusted to yield $S_{1,0}(p)|_{p=0.2M_n} = 1/2$.

tion for the high accuracy obtained from the Chebyshev expansion to this order. This particular solution, which will be shown to provide a good description of the electric form factors in Sec. 6, was obtained for the dipole form of the diquark amplitude, *i.e.*, from Eq. (2.15) with $n = 2$, using $m_q = 0.62M_n$ and $m_s = 0.7M_n$ (with $\sigma = \sigma' = 1/2$, $\eta = 1/3$). The value for the corresponding diquark width γ_2 , necessary to yield $\lambda = N_s^2$ (to an accuracy of 10^{-3}), resulted thereby to be $\gamma_2 = (0.294 M_n)^2$.

The dependence of the BS eigenvalue on the momentum partitioning parameter η is shown in Fig. 3.3. The complex domains of the constituent quark and diquark momentum variables, k_q^2 and k_s^2 respectively, that are sampled by the integration over the relative momentum k in the nucleon BSE are devoid of poles for $1 - m_s/M_n < \eta < m_q/M_n$. The pole in the momentum q^2 of the exchanged quark of the kernel in Eq. (3.6) is avoided by imposing the further bound $\eta > (1 - m_q/M_n)/2$ on the momentum partitioning parameter. Therefore, with the present choice of constituent masses it is for values of η in the range $0.3 < \eta < 0.6$, for which our numerical methods can yield stable results.

In principle, the integrations necessary to solve the nucleon BSE should always be real and never lead to an imaginary result (since $m_q + m_s > M_n$). More refined numerical methods would be necessary, however, when integrations were to be performed in presence of the poles in the constituent propagators that occur within the integration domain for values of η outside the above limits.

The momentum partitioning within the nucleon η is not an observable. Hence, for any value of η for which our numerical results are stable, we expect the eigenvalue of the nucleon BSE λ (which implicitly determines the nucleon mass) to be independent of η . In Fig. 3.3, the dependence on η of the nucleon BSE eigenvalue λ is explored using a fixed value for $\sigma = \sigma' = 1/2$ (solid curve) and using the values of σ and σ' from Eq. (3.13) (dashed curve).

In the first case, the arguments of the diquark amplitudes simplify to $x_i = -p_i^2$ with $p_1 = -(1 - 3\eta)P_n/2 + p + k/2$ and $p_2 = (1 - 3\eta)P_n/2 - k - p/2$. This implies that the real parts of x_i are guaranteed to be positive only for $\eta = 1/3$. For values of $\eta \neq 1/3$, a negative contribution arises from the timelike nucleon bound-state momentum P_n . If the n -pole forms for the diquark ampli-

tudes are employed, this results in the appearance of artificial poles whenever $(1 - 3\eta)^2 M_n^2/4 \geq \gamma_n$. The value of $\gamma_2 = (0.294 M_n)^2$ as it results here, would entail the appearance of a pole for $\eta \geq 0.53$. This explains why our numerical procedure becomes unstable as η approaches the value $1/2$ in this case.

No such timelike contribution to the x_i arises in the second case shown in Fig. 3.3. Here, for $\sigma = \sigma' = (1 - 2\eta)/(1 - \eta)$ the relative momenta p_i are independent of P_n , and there are no terms $\propto M_n^2$ in x_i ; see, for example, Eqs. (3.11,3.12). However, as $\eta \rightarrow 1/2$, we find that $\sigma, \sigma' \rightarrow 0$ and the diquark normalization integrals are then affected by singularities.

In the restricted range allowed to η , the results for the nucleon BSE obtained herein are found to be independent of η to very good accuracy when the equal momentum partitioning between the quark in the diquarks is used, $\sigma = \sigma' = 1/2$. In this case, the diquark normalization in Eq. (2.14) yields a fixed value for N_s^2 and any η dependence of the ratio λ/N_s^2 has to arise entirely from the nucleon BSE. The η independence of λ thus demonstrates that the solutions to the nucleon BSE are under good control.

The more considerable η -dependence observed for $\sigma = \sigma' = (1 - 2\eta)/(1 - \eta)$ arises from the dependence of N_s^2 on σ, σ' . Here, the limitations of the model assumptions for the *diquark* BS amplitudes are manifest. The dependence of the diquark BS amplitudes on the diquark bound-state mass, higher Chebyshev moments (which have been neglected) and the Lorentz structures (which we have neglected), are all responsible for this observed σ dependence. Such a dependence would not occur, had the diquark amplitudes employed herein been calculated from the diquark BSE.

For the numerical calculations of electromagnetic form factors presented in Sec. 5, we therefore choose to restrict the model to $\sigma = \sigma' = 1/2$ and vary η . From the observed independence of the nucleon BSE solutions to η (when $\sigma = \sigma' = 1/2$), one expects to find that calculated nucleon observables, such as the electromagnetic form factors, will display a similar independence of η as well.

Fixed width $S_1(p)|_{p=0.2M_n} = 1/2$, see Fig. 3.4:

| $P(x)$ | $m_s [M_n]$ | $m_q [M_n]$ | $\sqrt{\gamma} [M_n]$ | $g_s = 1/N_s$ |
|---------|-------------|-------------|-----------------------|---------------|
| $n = 1$ | 0.7 | 0.685 | 0.162 | 117.1 |
| $n = 2$ | 0.7 | 0.620 | 0.294 | 91.80 |
| $n = 4$ | 0.7 | 0.605 | 0.458 | 85.47 |
| $n = 6$ | 0.7 | 0.600 | 0.574 | 84.37 |
| $n = 8$ | 0.7 | 0.598 | 0.671 | 83.76 |
| EXP | 0.7 | 0.593 | 0.246 | 82.16 |
| GAU | 0.7 | 0.572 | 0.238 | 71.47 |

Fixed masses, see Fig. 3.5:

| | | | | |
|---------|-----|------|-------|-------|
| $n = 1$ | 0.7 | 0.62 | 0.113 | 155.8 |
| $n = 2$ | 0.7 | 0.62 | 0.294 | 91.80 |
| $n = 4$ | 0.7 | 0.62 | 0.495 | 81.08 |
| $n = 6$ | 0.7 | 0.62 | 0.637 | 78.61 |
| EXP | 0.7 | 0.62 | 0.283 | 74.71 |

Table 3.1. Summary of parameters used for the various diquark amplitudes $P(x)$, *c.f.*, Eqs. (2.15,2.16).

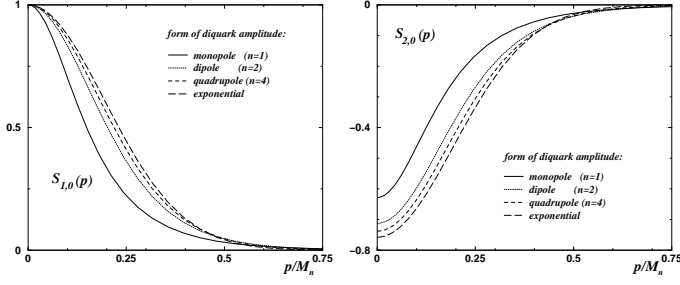


Fig. 3.5. The moments $S_{1,0}$ (left) and $S_{2,0}$ (right) of the nucleon amplitudes for the diquark amplitudes of Eqs. (2.15,2.16) with fixed masses, $m_s = 0.7M_n$, $m_q = 0.62M_n$.

In Figure 3.4 the zeroth Chebyshev moments $S_{1,0}(p)$ and $S_{2,0}(p)$ obtained from a numerical solution of the nucleon BSE with $\sigma = \sigma' = 1/2$ and $\eta = 1/3$ are shown, for various diquark amplitudes of the forms given in Eqs. (2.15) and Eq. (2.16) with $x_0 = 0$. To provide a comparison between these different forms of diquark BS amplitude, we have chosen to keep the diquark mass fixed and vary the quark mass until a solution of the nucleon BSE was found with the property that

$$S_{1,0}(p)|_{p=0.2M_n} \stackrel{!}{=} 1/2. \quad (3.24)$$

The resulting values for m_q along with the corresponding diquark widths and couplings $g_s \equiv 1/N_s$ are summarized in Table 3.1.

We observe that the mass of the quark required to satisfy the condition in Eq. (3.24) tends to smaller values for higher n -pole diquark amplitudes. On the other hand, for fixed constituent quark (and diquark) mass the higher n -pole diquark amplitudes lead to wider nucleon amplitudes. This is shown in Fig. 3.5 and the corresponding diquark widths and couplings are given in the lower part of Table 3.1. The mass values hereby correspond to the results shown in the previous Figure 3.4 for $n = 2$.

The qualitative effect of shifting the maximum in the Gaussian forms in Eq. (2.16) for the diquark amplitudes by a finite amount x_0 , is shown in Fig. 3.6. The curve for $x_0 = 0$ resembles the Gaussian result given in Fig. 3.4 with masses $m_s = 0.7M_n$ and $m_q = 0.572M_n$, which are kept fixed in the results for finite shifts x_0 . The corresponding widths and normalizations of these forms for the diquark amplitudes are given in Table 3.2. While the widths γ and the couplings g_s are not free parameters in our approach, the additional parameter x_0/γ_{GAU} introduced into the form of the diquark BS amplitude is free to vary. In contrast to the Gaussian form of the model diquark BS amplitude employed in Ref. [22] with $x_0/\gamma_{\text{GAU}} = 0.19/0.11 \simeq 1.73$, by implementing the diquark normalization condition, we find that the width must be about 30 times smaller to provide a sufficient interaction strength $g_s = 1/N_s^2$ necessary to bind the nucleon.

To provide for a closer comparison with the results of Ref. [22], we have also solved the nucleon BSE using the values of parameters employed in that study. That is, we have solved the nucleon BSE using $P_{\text{GAU}}(x)$ with the parameter $x_0/\gamma_{\text{GAU}} = 0.19/0.11$ and using the con-

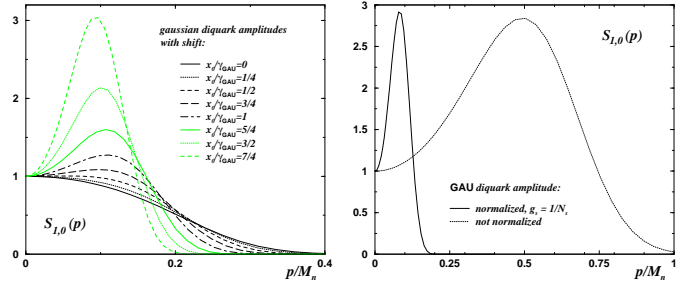


Fig. 3.6. The moment $S_{1,0}$ for the Gaussian diquark amplitudes of Eq. (2.16) with various shifts x_0/γ_{GAU} (left), see Table 3.2, and a comparison (right) of our result for $x_0/\gamma_{\text{GAU}} = 19/11$ (with $m_s = 0.7M_n$, $m_q = 0.555M_n$) with a result we obtain from using $\gamma_{\text{GAU}} = 0.11\text{GeV}^2$ as in Ref. [22].

stituent quark and diquark masses $m_q = 0.555M_n$ and $m_s = 0.7M_n$, respectively. (Note that we use the nucleon mass as the intrinsic momentum scale of our framework, whereas the momentum scale employed in Ref. [22] was 1 GeV.) The value employed in Ref. [22] for the diquark mass $m_s = 0.568$ GeV implies that $M_n = 811$ MeV in order to compare to our calculations (with $m_s = 0.7M_n$), and our value for the quark mass ($m_q = 0.555M_n$) thus corresponds to $m_q = 0.45$ GeV. With these parameters, we obtain $\gamma_{\text{GAU}} = (0.216 M_n)^2 = 0.308 \cdot 10^{-2}\text{GeV}^2$, which may be compared to $\gamma_{\text{GAU}} = (0.409 M_n)^2 = 0.11\text{GeV}^2$ used in Ref. [22].

| x_0/γ_{GAU} | $\sqrt{\gamma_{\text{GAU}}} [M_n]$ | $g_s = 1/N_s$ |
|---------------------------|------------------------------------|---------------|
| 0 | 0.238 | 71.47 |
| 1/4 | 0.209 | 69.09 |
| 1/2 | 0.181 | 72.64 |
| 3/4 | 0.154 | 81.96 |
| 1 | 0.130 | 97.75 |
| 5/4 | 0.109 | 121.3 |
| 3/2 | 0.091 | 154.3 |
| 7/4 | 0.077 | 198.5 |

Table 3.2. Width and normalizations of Gaussian amplitudes, Eq. (2.16) for various shifts x_0 , see Fig. 3.6 (right).

with $n = 2$ and $n = 4$ are employed, one obtains results for the electromagnetic form factors that are in good agreement with the phenomenological dipole fit for the electric proton form factor, while higher powers or exponential forms tend to produce form factors which decrease too fast with increasing momentum transfer Q^2 . We also show that use of a Gaussian form for the diquark BS amplitude with $x_0 \neq 0$ leads to neutron electric form factor that has a *qualitatively* different behavior than that obtained by using the other model forms of diquark BS amplitudes. Furthermore, this form leads to nodes in the neutron electric form factor for small Q^2 , a feature for which there is *no* experimental evidence.

The same results for the nucleon amplitudes as shown above are used for the calculations of the electromagnetic form factors of the proton and the neutron in Sec. 6. We will show that when n -pole diquark BS amplitudes

4 Normalization of Nucleon Bethe-Salpeter Amplitude

In order to reproduce the correct electromagnetic charges of the physical asymptotic states, here the proton and the neutron, a description of bound states requires that their Bethe-Salpeter (or Faddeev) amplitudes be properly normalized from the fully-interacting Green functions of the elementary fields. This is done according to the normalization conditions derived from *inhomogeneous* BS (or Faddeev) equations. In the present framework, the quark-diquark 4-point Green function is given by (suppressing Dirac indices)

$$G(p, q, P) = \left(G^{(0)-1}(p, q, P) - K(p, q, P) \right)^{-1}. \quad (4.1)$$

Here, $K(p, q, P)$ is the quark-exchange kernel of Eq. (3.6) depicted in Fig. 3, and $G^{(0)}(p, q, P)$ is the disconnected contribution to this Green function, given by

$$G_{\alpha\beta}^{(0)}(p, k, P) := (2\pi)^4 \delta^4(p - k) S_{\alpha\beta}(k_q) D(k_s) \delta_{\eta\eta'}, \quad (4.2)$$

with $k_q = \eta P + k$ and $k_s = (1-\eta)P - k$. Taking the derivative of $G(p, k, P)$ with respect to the total momentum P and then examining the leading contributions in the limit that $P^2 \rightarrow M_n^2$ which arise from the nucleon pole contribution from Eq. (3.1), one finds

$$M_n \Lambda^+(P_n) \stackrel{!}{=} i \int \frac{d^4 p}{(2\pi)^4} \frac{d^4 k}{(2\pi)^4} \quad (4.3)$$

$$\bar{\psi}(-p, P_n) \left(P_\mu \frac{\partial}{\partial P_\mu} G^{-1}(p, k, P) \right)_{P=P_n} \psi(k, P_n).$$

The most important difference in normalizing the amplitudes in the Bethe-Salpeter framework developed here and a genuine two-body BSE, is the dependence of the BS kernel on the total momentum of the bound-state P . In phenomenological studies of 2-body bound states BS kernels, such as ladder-approximate ones for example, are most commonly employed in a form which does not depend on the bound-state momentum. However, in the present approach, the original 3-body nature of the nucleon bound state *requires* the exchange kernel of the reduced BS equation for quark and diquark to depend on the total momentum P_n of the nucleon. In particular, when $\eta \neq 1/2$, the propagator for the exchanged quark in the kernel depends on the total momentum P_n and for $\eta \neq 1/3$, the diquark BS amplitudes depend on P_n . This added complication, which is easily avoided by ladder-approximate studies of meson bound states is unavoidable for studies of baryons. Thus, the normalization condition for the nucleon will always contain contributions from the derivative of the kernel.

Following the above procedure, one obtains a normalization condition of the form

$$1 \stackrel{!}{=} \eta N_q + (1 - \eta) N_D + (1 - 2\eta) N_X + (1 - 3\eta) N_P, \quad (4.4)$$

where

$$N_q = -\frac{P^\mu}{2M_n} i \int \frac{d^4 k}{(2\pi)^4} D(k_s) \quad (4.5)$$

$$\text{tr} \left[\bar{\psi}(-k, P) \left(\frac{\partial}{\partial k_q^\mu} S(k_q) \right) \tilde{\psi}(k, P) \right],$$

$$N_D = -\frac{P^\mu}{2M_n} i \int \frac{d^4 k}{(2\pi)^4} \left(\frac{\partial}{\partial k_s^\mu} D(k_s) \right) \quad (4.6)$$

$$\text{tr} \left[\bar{\psi}(-k, P) S(k_q) \tilde{\psi}(k, P) \right],$$

$$N_X = -\frac{P^\mu}{2M_n} i \int \frac{d^4 p}{(2\pi)^4} \frac{d^4 k}{(2\pi)^4} \frac{1}{2N_s^2} P(-p_1^2) P(-p_2^2) \quad (4.7)$$

$$\text{tr} \left[\bar{\psi}(-p, P) \left(\frac{\partial}{\partial q^\mu} S(q) \right) \psi(k, P) \right],$$

$$N_P = -\frac{P^\mu}{2M_n} i \int \frac{d^4 p}{(2\pi)^4} \frac{d^4 k}{(2\pi)^4} \frac{1}{2N_s^2} \quad (4.8)$$

$$\left(p_{1\mu} P'(-p_1^2) P(-p_2^2) - p_{2\mu} P(-p_1^2) P'(-p_2^2) \right)$$

$$\text{tr} \left[\bar{\psi}(-p, P) S(q) \psi(k, P) \right],$$

with $p_1 = -(1-3\eta)P/2 + p + k/2$, $p_2 = (1-3\eta)P/2 - p/2 - k$, for $\sigma = \sigma' = 1/2$.

It is clear from Eq. (4.4) that either the exchanged quark or the presence of a diquark substructure, or in general both, provide non-vanishing contributions to the nucleon BS normalization. Maintaining these terms is critical for the correct determination of the electromagnetic charges of baryons since the nucleon normalization and electromagnetic form factors are intimately related by the differential Ward identities.

In the following section, we show that in calculations of the electromagnetic form factors of the nucleon, use of the usual impulse approximation [42] (which includes only contributions arising from the coupling of the photon to the quark and diquark, that are related to the terms N_q and N_D in the normalization condition), by itself is insufficient to guarantee electromagnetic current and charge conservation of the nucleon.

One of the additional contributions required for the proper calculation of electromagnetic form factors that goes beyond the usual impulse approximation is the coupling of the photon to the exchanged-quark in the kernel from Eq. (3.5). We will show that this term provides a crucial contribution to the nucleon electromagnetic form factors and helps maintain electromagnetic current conservation of the nucleon. It is interesting to note that the contribution of this term is important even in the special case that $\eta = 1/2$ in which the term N_X does not contribute to the normalization condition of Eq. (4.4).

We will show in the next section that in the presence of a diquark with a non-trivial substructure, additional, direct couplings of the photon to this substructure are required to maintain current conservation. Owing to the occurrence of analogous terms in various different contexts [43, 44], these couplings will be referred to herein as ‘‘seagulls’’.

We conclude this section by summarizing that the respective contributions to the nucleon normalization condition of Eq. (4.4) given in Eqs. (4.5) to (4.6) correspond to the usual impulse approximate contributions arising from the constituent quark and diquark, plus the contribution from the exchange-quark in the BS kernel, and the seagull contributions which arise from the quark-substructure in the diquark correlations.

5 The Electromagnetic Current in Impulse Approximation and Beyond

The electromagnetic current operator $J_\mu^{\text{em}}(x)$ in impulse approximation is determined by the disconnected contributions from the electromagnetic couplings of the spectator quark (J_q^μ) and the scalar diquark (J_D^μ) which in the Mandelstam formalism are calculated from the following momentum space kernels [42],

$$J_q^\mu(p, P'; k, P) = (2\pi)^4 \delta^4(p - k - \hat{\eta}Q) \quad (5.1)$$

$$q_q \Gamma_q^\mu(\eta P' + p, \eta P + k) D^{-1}(\hat{\eta}P - k),$$

$$J_D^\mu(p, P'; k, P) = (2\pi)^4 \delta^4(p - k + \eta Q) \quad (5.2)$$

$$q_D \Gamma_D^\mu(\hat{\eta}P' - p, \hat{\eta}P - k) S^{-1}(\eta P + k),$$

with $Q = P' - P$ and $\eta + \hat{\eta} = 1$. The charge of the spectator quark in the nucleon is denoted q_q , the charge of the scalar diquark is q_D , and $q_q + q_D = 1$ and 0 for the proton and neutron, respectively. The Ward-Takahashi identities for the quark and diquark electromagnetic vertices are

$$Q_\mu \Gamma_q^\mu(p + Q, p) = iS^{-1}(p + Q) - iS^{-1}(p), \quad (5.3)$$

$$Q_\mu \Gamma_D^\mu(p + Q, p) = iD^{-1}(p + Q) - iD^{-1}(p). \quad (5.4)$$

From these one can immediately write down the nucleon matrix elements for the divergences of the corresponding Mandelstam currents between initial and final nucleon states with momentum and spin P, s and P', s' respectively, as

$$\langle P', s' | \partial_\mu J_q^\mu(0) | P, s \rangle = q_q \int \frac{d^4 k}{(2\pi)^4} \left\{ \quad (5.5)$$

$$\begin{aligned} & \bar{u}(P', s') \tilde{\psi}(-k + \hat{\eta}Q, P') \psi(k, P) u(P, s) \\ & - \bar{u}(P', s') \tilde{\psi}(-k + \hat{\eta}Q, P') \tilde{\psi}(k, P) u(P, s) \end{aligned} \Big\},$$

$$\langle P', s' | \partial_\mu J_D^\mu(0) | P, s \rangle = q_D \int \frac{d^4 k}{(2\pi)^4} \left\{ \quad (5.6)$$

$$\begin{aligned} & \bar{u}(P', s') \tilde{\psi}(-k - \eta Q, P') \psi(k, P) u(P, s) \\ & - \bar{u}(P', s') \tilde{\psi}(-k - \eta Q, P') \tilde{\psi}(k, P) u(P, s) \end{aligned} \Big\}.$$

Here, we insert the BSEs for the amplitudes $\tilde{\psi}$ and $\tilde{\tilde{\psi}}$ which can be written in the compact form,

$$\tilde{\psi}(p, P) = \int \frac{d^4 k}{(2\pi)^4} K(p, k, P) \psi(p, P), \quad (5.7)$$

$$\tilde{\tilde{\psi}}(-p, P) = \int \frac{d^4 k}{(2\pi)^4} \tilde{\psi}(-k, P) K(p, k, P). \quad (5.8)$$

After shifting the integration momentum by $p + \hat{\eta}Q \rightarrow p$ in the second terms of Eqs. (5.5) and (5.6), one obtains,

$$\langle P', s' | \partial_\mu J_q^\mu(0) | P, s \rangle = q_q \int \frac{d^4 p}{(2\pi)^4} \frac{d^4 k}{(2\pi)^4} \left\{ \quad (5.9)$$

$$\begin{aligned} & \bar{u}(P', s') \tilde{\psi}(-p, P') K(p, k + \hat{\eta}Q, P') \psi(k, P) u(P, s) \\ & - \bar{u}(P', s') \tilde{\psi}(-p, P') K(p - \hat{\eta}Q, k, P) \psi(k, P) u(P, s) \end{aligned} \Big\},$$

$$\langle P', s' | \partial_\mu J_D^\mu(0) | P, s \rangle = q_D \int \frac{d^4 p}{(2\pi)^4} \frac{d^4 k}{(2\pi)^4} \left\{ \quad (5.10)$$

$$\begin{aligned} & \bar{u}(P', s') \tilde{\psi}(-p, P') K(p, k - \eta Q, P') \psi(k, P) u(P, s) \\ & - \bar{u}(P', s') \tilde{\psi}(-p, P') K(p + \eta Q, k, P) \psi(k, P) u(P, s) \end{aligned} \Big\}.$$

Examination of the terms in Eqs. (5.9) and (5.10) reveals that their sum gives rise to a conserved current only if $K(p, k, P) \equiv K(p - k)$. That is, if the nucleon BS kernel is independent of the total nucleon bound-state momentum P and, in addition, it only depends on the *difference* of the relative momenta $p - k$. These criteria are satisfied in studies of meson bound states within the ladder approximation, see for example Ref. [33]. However, we observe that even in absence of an explicit dependence on the total nucleon momentum P , the exchange kernel of the BSE, as obtained from the nucleon Faddeev equation, *necessarily* depends on the sum of the relative momenta $p + k$ and not the difference. It follows from this that already to this level of the approximation which corresponds to neglecting diquark substructure together with using $\eta = 1/2$ as in Refs. [35, 36], the electromagnetic current of the nucleon is not conserved in the impulse approximation and it is necessary to include an additional coupling of the photon to the quark-exchange kernel.

It is interesting to note that similar photon-kernel couplings are required in other systems as well. For example, while the nucleon-nucleon scattering kernels due to meson exchanges depend only on the difference of the relative momenta (*i.e.*, $K \equiv K(p - k)$), the isospin dependence of a charged meson that is exchanged between the two nucleons requires one to introduce additional photon couplings to the exchanged meson to maintain current conservation, in this case the charged pion. Such contributions play an important role in determining the electromagnetic form factors of the deuteron [45].

The coupling of the exchange quark (with electromagnetic charge q_X) in the kernel of Eq. (3.5) gives rise to the additional contribution J_X to the nucleon current:

$$J_X^\mu(p, P'; k, P) = -q_X \frac{1}{2} \quad (5.11)$$

$$\tilde{\chi}(p_1, \hat{\eta}P - k) S^T(q) \Gamma_q^{\mu T}(q', q) S^T(q') \tilde{\chi}^T(p_2', \hat{\eta}P' - p),$$

with $q = \hat{\eta}P - \eta P' - p - k$, $q' = q + Q$,

$$p_1 = \sigma(\eta P' + p) - \hat{\sigma}q, \quad p_2' = -\sigma'(\eta P + k) + \hat{\sigma}'q',$$

and $\sigma + \hat{\sigma} = \sigma' + \hat{\sigma}' = 1$.

From the Ward-Takahashi identity for the quark-photon vertex in Eq. (5.3), one finds that the divergence of the exchanged-quark contribution to the nucleon electromag-

netic current is

$$Q_\mu J_X^\mu(p, P'; k, P) = \quad (5.12)$$

$$-iq_X \frac{1}{2} \left(\tilde{\chi}(p_1, \hat{\eta}P - k) S^T(q) \tilde{\chi}^T(p'_2, \hat{\eta}P' - p) \right. \\ \left. - \tilde{\chi}(p_1, \hat{\eta}P - k) S^T(q') \tilde{\chi}^T(p'_2, \hat{\eta}P' - p) \right).$$

To provide a comparison with the quark and diquark electromagnetic currents given above for the quark-exchange kernel of Eq. (3.5) written using the same momentum conventions as used in Eq. (5.11), we rewrite the divergences of the Mandelstam currents given in Eqs. (5.9) and (5.10) as

$$Q_\mu J_q^\mu(p, P'; k, P) = \quad (5.13)$$

$$-iq_q \frac{1}{2} \left(\tilde{\chi}(p_1, \hat{\eta}P - k) S^T(q) \tilde{\chi}^T(p'_2 - Q, \hat{\eta}P' - p) \right. \\ \left. - \tilde{\chi}(p_1 - Q, \hat{\eta}P - k) S^T(q') \tilde{\chi}^T(p'_2, \hat{\eta}P' - p) \right),$$

$$Q_\mu J_D^\mu(p, P'; k, P) = \quad (5.14)$$

$$-iq_D \frac{1}{2} \left(\tilde{\chi}(p_1 - \hat{\sigma}Q, \hat{\eta}P - k + Q) S^T(q') \tilde{\chi}^T(p'_2, \hat{\eta}P' - p) \right. \\ \left. - \tilde{\chi}(p_1, \hat{\eta}P - k) S^T(q) \tilde{\chi}^T(p'_2 - \hat{\sigma}'Q, \hat{\eta}P' - p - Q) \right).$$

Since $q_q - q_D + q_X = 0$, one thus finds that, in the case of a point-like diquark BS amplitude, (*i.e.*, neglecting any momentum dependence in the diquark BS amplitudes $\tilde{\chi}$ and $\tilde{\tilde{\chi}}$), the sum of the three currents given above now yields a conserved electromagnetic current for the nucleon; that is,

$$Q_\mu \left(J_q^\mu + J_D^\mu + J_X^\mu \right) = 0. \quad (5.15)$$

For this cancellation all three contributions are crucial. In particular, the contributions from the photon coupling to the exchanged quark J_X^μ , as well as the impulse approximate contributions $J_q^\mu + J_D^\mu$ must all be included.

However, if the substructure of the diquark BS amplitudes is taken into account and the diquark BS amplitude has a dependence on any momentum, this cancellation is destroyed. The violations to current conservation can be displayed in the present framework in a way which will become useful in following sections. Rearranging the six terms above in such a way to factor out two terms,

$$S_1(p, P'; k, P) := -iq_q \tilde{\chi}(p_1 - Q, \hat{\eta}P - k) + \quad (5.16)$$

$$iq_D \tilde{\chi}(p_1 - \hat{\sigma}Q, \hat{\eta}P - k + Q) - iq_X \tilde{\chi}(p_1, \hat{\eta}P - k),$$

$$S_2(p, P'; k, P) := -iq_q \tilde{\tilde{\chi}}(p'_2 - Q, \hat{\eta}P' - p) + \quad (5.17)$$

$$iq_D \tilde{\tilde{\chi}}(p'_2 - \hat{\sigma}'Q, \hat{\eta}P' - p - Q) - iq_X \tilde{\tilde{\chi}}(p'_2, \hat{\eta}P' - p),$$

one obtains

$$Q_\mu \left(J_q^\mu + J_D^\mu + J_X^\mu \right) = \quad (5.18)$$

$$-\frac{1}{2} \left(S_1(p, P'; k, P) S^T(q') \tilde{\chi}^T(p'_2, \hat{\eta}P' - p) \right. \\ \left. - \tilde{\chi}(p_1, \hat{\eta}P - k) S^T(q) S_2^T(p, P'; k, P) \right).$$

It will be demonstrated in the subsection below that these contributions are exactly canceled by the so-called ‘‘seagull’’ contributions which arise from one-particle irreducible 4-point couplings of the two quarks, the diquark and photon. Such terms must be included whenever the substructure of a diquark bound state (in form of momentum-dependent diquark BS amplitude) is included in the description of the nucleon. It is interesting to note that such seagull contributions are also known to be necessary for γ -meson-baryon-baryon couplings in order to satisfy the corresponding Ward-Takahashi identities [43, 44].

5.1 Ward Identities and Seagulls

The Ward-Takahashi identity for the quark-photon vertex, Eq. (5.3), follows from the equal-time commutation relation for the electromagnetic quark-current operator $j_\mu(x)$ with the quark field (with charge q_q),

$$[j^0(x), q(y)] \delta(x_0 - y_0) = -q_q q(x) \delta^4(x - y), \\ [j^0(x), \bar{q}(y)] \delta(x_0 - y_0) = q_q \bar{q}(x) \delta^4(x - y). \quad (5.19)$$

Formal problems with equal-time commutation relations for interacting fields can be avoided by replacing the canonical formalism with a Lagrangian formulation based on relativistic causality rather than to single out a sharp time-like surface [46, ?]. However, as an operational device for the derivation of Ward identities, the equal-time commutation relations of Eqs. (5.19) will nevertheless give the correct result.

Consider the 5-point Green function that describes the photon coupling to four quarks $G_{\alpha\gamma,\beta\delta}^\mu$. Using the notation that $q_{q\alpha}$, $q_{q\beta}$, $q_{q\gamma}$, and $q_{q\delta}$ denote the charges of the quark fields with Dirac indices denoted by α , β , γ and δ , respectively, the Ward identity is given by

$$\partial_\mu^z \langle T(q_\gamma(x_3) q_\alpha(x_1) \bar{q}_\beta(x_2) \bar{q}_\delta(x_4) j^\mu(z)) \rangle = \quad (5.20)$$

$$- (q_{q\alpha} \delta^4(x_1 - z) + q_{q\gamma} \delta^4(x_3 - z) - q_{q\beta} \delta^4(x_2 - z) \\ - q_{q\delta} \delta^4(x_4 - z)) \langle T(q_\gamma(x_3) q_\alpha(x_1) \bar{q}_\beta(x_2) \bar{q}_\delta(x_4)) \rangle.$$

The 4-point function on the right-hand side has the diquark pole contribution given in Eq. (2.2) and depicted in Fig. 2. The Fourier transformation of the left-hand side of Eq. (5.20) allows one to define,

$$G_{\alpha\gamma,\beta\delta}^\mu(p, P'; k, P) := \quad (5.21)$$

$$\int d^4x_1 d^4x_2 d^4x_3 d^4x_4 e^{ip_\alpha x_1} e^{ip_\beta x_2} e^{ip_\gamma x_3} e^{ip_\delta x_4} \\ \langle T(q_\gamma(x_3) q_\alpha(x_1) \bar{q}_\beta(x_2) \bar{q}_\delta(x_4) j^\mu(0)) \rangle.$$

Here, $p = \sigma p_\gamma - \hat{\sigma} p_\alpha$, $k = \sigma' p_\beta - \hat{\sigma}' p_\delta$ and $P' = P + Q$ as before. It is straight forward to verify the following Ward identity for this 5-point Green function from the pole contribution to the 4-quark Green function, given in Eq. (2.2), which determines the dominant contribution when the diquark momenta are close to the diquark pole

at $P^2 = P'^2 = m_s^2$.

$$\begin{aligned}
iQ_\mu G_{\alpha\gamma,\beta\delta}^\mu(p, P'; k, P) := & \quad (5.22) \\
& q_{q\alpha} \frac{i}{P^2 - m_s^2 + i\epsilon} \chi_{\gamma\alpha}(p + \hat{\sigma}Q, P) \bar{\chi}_{\beta\delta}(k, P) \\
& + q_{q\gamma} \frac{i}{P^2 - m_s^2 + i\epsilon} \chi_{\gamma\alpha}(p - \sigma Q, P) \bar{\chi}_{\beta\delta}(k, P) \\
& - q_{q\beta} \frac{i}{P'^2 - m_s^2 + i\epsilon} \chi_{\gamma\alpha}(p, P') \bar{\chi}_{\beta\delta}(k - \sigma'Q, P') \\
& - q_{q\delta} \frac{i}{P'^2 - m_s^2 + i\epsilon} \chi_{\gamma\alpha}(p, P') \bar{\chi}_{\beta\delta}(k + \hat{\sigma}'Q, P').
\end{aligned}$$

To explicitly demonstrate that this does indeed give the additional contributions necessary to current conservation of the BSE solution for the nucleon, one needs to consider the irreducible 4-point coupling of the photon to the quarks and the diquark derived from the following definition:

$$\begin{aligned}
(S(p_\gamma) M^\mu(p_\gamma, p_\alpha, P_d) S^T(p_\alpha))_{\gamma\alpha} D(P_d) := & \quad (5.23) \\
Z^{-1} \int \frac{d^4k}{(2\pi)^4} G_{\alpha\gamma,\beta\delta}^\mu(p, P_d + Q; k, P_d) \tilde{\chi}_{\delta\beta}(k, P_d),
\end{aligned}$$

with $p_\alpha = -p + \sigma(P_d + Q)$, $p_\gamma = p + \hat{\sigma}(P_d + Q)$, and

$$Z := \int \frac{d^4k}{(2\pi)^4} \text{tr}[\tilde{\chi}(k, P_d) \tilde{\chi}(k, P_d)]. \quad (5.24)$$

The Ward identity for the 5-point Green function then entails,

$$\begin{aligned}
iQ_\mu M^\mu(p_\gamma, p_\alpha, P_d) = & \quad (5.25) \\
& q_{q\alpha} \tilde{\chi}(p + \hat{\sigma}Q, P_d) S^T(p_\alpha - Q) S^{-1T}(p_\alpha) \\
& + q_{q\beta} S^{-1}(p_\gamma) S(p_\gamma - Q) \tilde{\chi}(p - \sigma Q, P_d) \\
& - \Delta_\Phi(Q^2) \tilde{\chi}(p, P_d + Q) \frac{P_d^2 - m_s^2}{(P_d + Q)^2 - m_s^2 + i\epsilon},
\end{aligned}$$

with

$$Q = p_\gamma + p_\alpha - P_d, \quad p = \sigma p_\gamma - \hat{\sigma} p_\alpha,$$

($\sigma + \hat{\sigma} = 1$) and $\Delta_\Phi(Q^2)$ is defined by

$$\begin{aligned}
\Delta_\Phi(Q^2) := Z^{-1} \int \frac{d^4k}{(2\pi)^4} \{ & \quad (5.26) \\
& q_{q\beta} \text{tr}[S^T(-k + \hat{\sigma}'P_d + Q) \times \\
& \quad \tilde{\chi}(k - \sigma'Q, P_d + Q) S(k + \sigma'P_d) \tilde{\chi}(k, P_d)] \\
& + q_{q\delta} \text{tr}[S^T(-k + \hat{\sigma}'P_d) \times \\
& \quad \tilde{\chi}(k + \hat{\sigma}'Q, P_d + Q) S(k + \sigma'P_d + Q) \tilde{\chi}(k, P_d)] \}.
\end{aligned}$$

In the limit $Q \rightarrow 0$, this is normalized in such a way as to yield the charge of the scalar diquark; that is, $\Delta_\Phi(0) = q_{q\beta} + q_{q\delta} \equiv q_\Phi$.

In a more detailed and complete calculation, the coupling of the diquark to the photon would itself have to be done within a Mandelstam formalism. To achieve this, the Ward identity of Eq. (5.3) would be used in the Mandelstam formalism to construct the Ward identity for the quark substructure of the diquark, thereby replacing the

naive Ward identity of Eq. (5.4) with a more accurate identity which accurately depicts the quark substructure of the diquark. This added complication can be worked out in a straight-forward manner by introducing a few additional technical details. However, the basic principle of such couplings, as derived from Ward identities, can be seen from the following simplifying assumption, which will be used in the following sections. Assume that $\Delta_\Phi(Q^2)$ is independent of the photon momentum, such that $\Delta_\Phi(Q^2) = \Delta_\Phi(0) = q_\Phi$. This assumption is sufficient in order to obtain the correct charges for the nucleon bound state. From this starting point, the electromagnetic diquark form factor can be easily included in a minor extension of the framework and follows simply from the inclusion of a dependence on the photon momentum Q^2 of $\Delta_\Phi(Q^2)$.

By including the effect of only the charge of the diquark, that is setting $\Delta_\Phi(Q^2) \equiv q_\Phi$ for all photon momenta Q , the divergence of the amplitude M^μ is written as

$$\begin{aligned}
Q_\mu M^\mu(p_\alpha, p_\beta, P_d) = & \quad (5.27) \\
& Q^\mu M_\mu^{legs}(p_\alpha, p_\beta, P_d) + Q^\mu M_\mu^{sg}(p_\alpha, p_\beta, P_d),
\end{aligned}$$

where M^{legs} contains the couplings of the photon to the amputated quark and diquark legs according to their respective Ward identities,

$$\begin{aligned}
iQ^\mu M_\mu^{legs}(p_\alpha, p_\beta, P_d) = & \quad (5.28) \\
& q_{q\alpha} (S^{-1}(p_\alpha) - S^{-1}(p_\alpha - Q)) \times \\
& \quad S(p_\alpha - Q) \tilde{\chi}(p - \hat{\sigma}Q, P_d) \\
& + q_{q\beta} \tilde{\chi}(p + \sigma Q, P_d) S^T(p_\beta - Q) \times \\
& \quad (S^{-1T}(p_\beta) - S^{-1T}(p_\beta - Q)) \\
& - q_\Phi \tilde{\chi}(p, P_d + Q) D(P_d + Q) \\
& \quad (D^{-1}(P_d) - D^{-1}(P_d + Q)),
\end{aligned}$$

where the term M^{sg} describes the one-particle irreducible seagull couplings and its divergence is given by

$$\begin{aligned}
iQ^\mu M_\mu^{sg}(p_\alpha, p_\beta, P_d) = & \quad (5.29) \\
& q_{q\alpha} \tilde{\chi}(p - \hat{\sigma}Q, P_d) + q_{q\beta} \tilde{\chi}(p + \sigma Q, P_d) \\
& \quad - q_\Phi \tilde{\chi}(p, P_d + Q).
\end{aligned}$$

These seagull couplings are exactly what is needed to arrive at a conserved electromagnetic current for the nucleon. Upon substitution of the charges of the spectator and exchanged quark and the scalar diquark, $q_{q\alpha} = q_q$, $q_{q\beta} = q_X$ and $q_\Phi = q_D$, respectively, one finds

$$S_1(p, P'; k, P) = Q^\mu M_\mu^{sg}(\eta P' + p, q + Q, \eta P - k), \quad (5.30)$$

with $Q = P' - P$. A solution to this Ward identity, with transverse terms added so as to keep the limit $Q \rightarrow 0$ regular, which follows from a standard construction, *c.f.*, Refs. [43, 44], is provided by

$$iM_\mu^{sg}(p_\alpha, p_\beta, P_d) = \quad (5.31)$$

$$\begin{aligned}
& q_q \frac{(2p_\alpha - Q)_\mu}{p_\alpha^2 - (p_\alpha - Q)^2} \left(\tilde{\chi}(p_\alpha - Q, p_\beta, P_d) - \tilde{\chi}(p_\alpha, p_\beta, P_d) \right) \\
& + q_X \frac{(2p_\beta - Q)_\mu}{p_\beta^2 - (p_\beta - Q)^2} \left(\tilde{\chi}(p_\alpha, p_\beta - Q, P_d) - \tilde{\chi}(p_\alpha, p_\beta, P_d) \right) \\
& - q_D \frac{(2P_d + Q)_\mu}{(P_d + Q)^2 - P_d^2} \left(\tilde{\chi}(p_\alpha, p_\beta, P_d + Q) - \tilde{\chi}(p_\alpha, p_\beta, P_d) \right)
\end{aligned}$$

with $Q = p_\alpha + p_\beta - P_d$. Analogously, for the other seagull, one finds

$$i\bar{M}_\mu^{sg}(p_\alpha, p_\beta, P_d) = \quad (5.32)$$

$$q_q \frac{(2p_\alpha - Q)_\mu}{p_\alpha^2 - (p_\alpha - Q)^2} \left(\tilde{\chi}(p_\alpha - Q, p_\beta, P_d) - \tilde{\chi}(p_\alpha, p_\beta, P_d) \right)$$

$$+ q_X \frac{(2p_\beta - Q)_\mu}{p_\beta^2 - (p_\beta - Q)^2} \left(\tilde{\chi}(p_\alpha, p_\beta - Q, P_d) - \tilde{\chi}(p_\alpha, p_\beta, P_d) \right)$$

$$- q_D \frac{(2P_d - Q)_\mu}{P_d^2 - (P_d - Q)^2} \left(\tilde{\chi}(p_\alpha, p_\beta, P_d - Q) - \tilde{\chi}(p_\alpha, p_\beta, P_d) \right).$$

The amplitudes $\tilde{\chi}(p_\alpha, p_\beta, P_d)$ herein need to be constructed from the BS amplitude of the scalar diquark by removing the overall momentum conserving constraint $p_\alpha + p_\beta = P_d$. With these seagull couplings, a conserved electromagnetic current operator is obtained by including the seagull contribution

$$J_\mu^{sg}(p, P'; k, P) = \quad (5.33)$$

$$\frac{1}{2} \left(M_\mu^{sg}(\eta P' + p, q', \hat{\eta}P - k) S^T(q') \tilde{\chi}^T(p_2, \hat{\eta}P' - p) \right.$$

$$\left. - \tilde{\chi}(p_1, \hat{\eta}P - k) S^T(q) \bar{M}_\mu^{sg T}(-(\eta P + k), -q, \hat{\eta}P' - p) \right).$$

The total conserved electromagnetic current of the nucleon is therefore given by $J_{em}^\mu := J_q^\mu + J_D^\mu + J_X^\mu + J_{sg}^\mu$.

Technically, the additional contributions to the electromagnetic nucleon current arising from exchanged quark in the nucleon BSE kernel J_X^μ , as well as the seagull term J_{sg}^μ , involve two 4-dimensional loop integrations to calculate the electromagnetic form factors from the nucleon BS amplitudes. As demonstrated above, this considerable extension to the Mandelstam formalism (involving only single loop integrations) is absolutely necessary to correctly include the non-trivial substructure of the diquark correlations and maintain current conservation of the nucleon.

While seagull contributions are not necessary in a framework that employs point-like diquarks, as is the case in Ref. [35], beyond-impulse contributions, such as the coupling of the exchanged-quark to the photon are necessary! In the study of Ref. [35], it was observed that neglecting this contribution produced negligible violations to the charges of proton and neutron and so it was dismissed as unimportant. However, in the case of the present study this contribution is significant. The reason for this is the larger value of the coupling strength g_s (obtained from the diquark normalization condition $g_s = 1/N_s^2$) used herein. For a point-like diquark, the coupling need not be as large. Furthermore, in contrast to the impulse-approximate Mandelstam currents, which are independent of g_s , the contribution to the electromagnetic current due to the exchanged quark is proportional to g_s^2 (see Eq. (5.11)). Hence, use of a smaller coupling strength g_s^2 in the BSE, reduces the importance of going beyond the impulse approximation.

As an example of the importance of the contributions beyond the impulse terms of J_q and J_D , we consider the results for the proton and neutron electromagnetic charges using the amplitudes plotted in Fig. 3.2 from the Mandelstam current $J_q^\mu + J_D^\mu$ alone. This leads to charges

$Q_P = 0.85$ for the proton and $Q_N = 0.15$ for the neutron. A theorem constrains the charges of the proton and neutrons to obey $Q_P + Q_N = 1$. The theorem relies on using $\eta = 1/3$ and is derived from the nucleon normalization condition in Eq. (4.4). However, the way it is realized here is not very satisfying. In Sec. 6, we discuss in detail the relevance of the various contributions to the electromagnetic form factors of the proton and neutron due to exchanged-quark-photon coupling and seagull couplings.

Having proven that the present framework conserves the electromagnetic current, one might think that the results for the proton and neutron charges, $Q_P = 1$ and $Q_N = 0$, must follow trivially. However, the verification that this framework provides the correct charges for the proton and neutron is not trivial as demonstrated in the next section.

For finite momentum transfer $Q = P' - P > 0$, the complete Mandelstam couplings for the diquark will still require modifications. If the photon is coupled to the elementary carriers of charge only, that is, to the quarks within the diquark (with quark charges $q_{q\alpha}$, $q_{q\beta}$), the photon-diquark vertex will itself be of the form,

$$F_\phi^\mu(Q) = \quad (5.34)$$

$$Z^{-1} q_{q\alpha} \int \frac{d^4 k}{(2\pi)^4} \text{tr} \left[S^T(-k + \hat{\sigma}P_d + Q) \times \right.$$

$$\tilde{\chi}(k - \sigma Q, P_d + Q) S(k + \sigma P_d) \tilde{\chi}(k, P_d) \times$$

$$\left. S^T(-k + \hat{\sigma}P_d) \Gamma^{\mu T}(-k + \hat{\sigma}P_d + Q, -k + \hat{\sigma}P_d) \right]$$

$$+ Z^{-1} q_{q\beta} \int \frac{d^4 k}{(2\pi)^4} \text{tr} \left[S^T(-k + \hat{\sigma}P_d) \times \right.$$

$$\tilde{\chi}(k + \hat{\sigma}'Q, P_d + Q) S(k + \sigma P_d + Q) \times$$

$$\left. \Gamma^\mu(k + \sigma P_d + Q, k + \sigma P_d) S(k + \sigma P_d) \tilde{\chi}(k, P_d) \right].$$

This gives the correct diquark charge in the limit the photon momentum $Q \rightarrow 0$. In this limit, as far as the electric form factors of the nucleons are concerned this detail is irrelevant since they are constrained to be proportional to the charge of the nucleon. However, the anomalous magnetic moments of then nucleon may receive important contributions from the quark substructure of the diquark, which would otherwise have to be modeled by an ad-hoc *anomalous magnetic moment* for the scalar diquark.

6 Electromagnetic Form Factors of the Nucleon

The matrix elements of the nucleon current can be parametrized as

$$\langle P', s' | J_{em}^\mu(0) | P, s \rangle = \quad (6.1)$$

$$\bar{u}(P', s') \left[\gamma^\mu \mathcal{F}_1 + \frac{i\kappa \mathcal{F}_2}{2M} \sigma^{\mu\nu} Q_\nu \right] u(P, s).$$

Here, \mathcal{F}_1 and \mathcal{F}_2 are the Dirac charge and the Pauli anomalous magnetic form factors, respectively [47]. $Q^\mu = P' - P$

is the spacelike momentum of the virtual photon probing the nucleon ($-Q^2 \geq 0$). Using the Gordon decomposition

$$\bar{u}(P', s') \frac{i\sigma^{\mu\nu} Q_\nu}{2M} u(P, s) = \bar{u}(P', s') \left[\gamma^\mu - \frac{P_{\text{BF}}^\mu}{M} \right] u(P, s), \quad (6.2)$$

with the definition of the Breit momentum $P_{\text{BF}} := (P' + P)/2$, the current can be rewritten as

$$\langle P', s' | J_{\text{em}}^\mu(0) | P, s \rangle = \bar{u}(P', s') \left[\gamma^\mu (\mathcal{F}_1 + \kappa \mathcal{F}_2) - \frac{P_{\text{BF}}^\mu}{M} \kappa \mathcal{F}_2 \right] u(P, s). \quad (6.3)$$

It is convenient in the following to introduce (matrix valued) matrix elements by initial and final spin-summations,

$$\langle P' | \hat{J}^\mu | P \rangle := \langle P', s' | J^\mu | P, s \rangle \sum_{s, s'} u(P', s') \bar{u}(P, s), \quad (6.4)$$

to remove the nucleon spinors. The frequently used Sachs electric and magnetic form factors G_E and G_M , are introduced via

$$G_E = \mathcal{F}_1 + \frac{Q^2}{4M^2} \kappa \mathcal{F}_2, \quad (6.5)$$

$$G_M = \mathcal{F}_1 + \kappa \mathcal{F}_2. \quad (6.6)$$

These can be extracted from Eq. (6.4),

$$\langle P' | \hat{J}_{\text{em}}^\mu(0) | P \rangle = \Lambda^+(P') \left[\gamma^\mu G_M + M \frac{P_{\text{BF}}^\mu}{P_{\text{BF}}^2} (G_E - G_M) \right] \Lambda^+(P), \quad (6.7)$$

by taking traces of $\langle \hat{J}_{\text{em}}^\mu \rangle \equiv \langle P' | \hat{J}_{\text{em}}^\mu(0) | P \rangle$ as follows:

$$G_E = \frac{M}{2P_{\text{BF}}^2} \text{tr} \langle \hat{J}_{\text{em}}^\mu \rangle P_{\text{BF}}^\mu, \quad (6.8)$$

$$G_M = \frac{M^2}{Q^2} \left(\text{tr} \langle \hat{J}_{\text{em}}^\mu \rangle \gamma^\mu - \frac{M}{P_{\text{BF}}^2} \text{tr} \langle \hat{J}_{\text{em}}^\mu \rangle P_{\text{BF}}^\mu \right). \quad (6.9)$$

We calculate the current matrix elements using Mandelstam's approach with the current operators defined in the previous sections, such that

$$\langle P' | \hat{J}_{\text{em}}^\mu(0) | P \rangle = \int \frac{d^4 p}{(2\pi)^4} \frac{d^4 k}{(2\pi)^4} \bar{\psi}(-p, P') J_{\text{em}}^\mu(p, P'; k, P) \psi(k, P) \quad (6.10)$$

The current operator J_{em}^μ consists of the four parts which describe the coupling of the photon to quark or diquark, to the exchanged-quark and the seagull contributions which arise from the coupling of the photon to the diquark BS amplitudes. These are determined by the following kernels,

$$J_q^\mu = q_q \Gamma_q^\mu(p_q, k_q) D^{-1}(k_s) (2\pi)^4 \delta^4(p - k - \hat{\eta}Q), \quad (6.11)$$

$$J_D^\mu = q_D \Gamma_D^\mu(p_s, k_s) S^{-1}(k_q) (2\pi)^4 \delta^4(p - k + \eta Q), \quad (6.12)$$

$$J_X^\mu = -q_X \frac{1}{2} \quad (6.13)$$

$$\tilde{\chi}(p_1, k_s) S^T(q) \Gamma_q^{\mu T}(q', q) S^T(q') \tilde{\chi}^T(p_2', p_s),$$

$$J_{sg}^\mu = \frac{1}{2} \left(M_{sg}^\mu(p_q, q', k_s) S^T(q') \tilde{\chi}^T(p_2', p_s) - \tilde{\chi}(p_1, k_s) S^T(q) \bar{M}_{sg}^{\mu T}(-k_q, -q, p_s) \right). \quad (6.14)$$

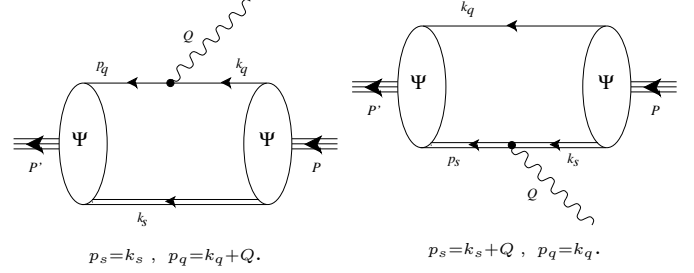


Fig. 6.1. Impulse approximation diagrams.

The abbreviations for the various momenta are summarized in the following table:

| | incoming | outgoing |
|---------------------|--------------------------------------|---------------------------------------|
| quark: | $k_q = \eta P + k$ | $p_q = \eta P' + p$ |
| diquark: | $k_s = \hat{\eta} P - k$ | $p_s = \hat{\eta} P' - p$ |
| exchange quark: | $q = \hat{\eta} P - \eta P' - p - k$ | $q' = \hat{\eta} P' - \eta P - p - k$ |
| relative momenta | $(\sigma = \sigma' = 1/2)$ | |
| within diquark: | $p_1 = \frac{1}{2} (p_q - q)$ | $p_2' = \frac{1}{2} (-k_q + q')$ |
| seagull quark-pair: | $p_1' = \frac{1}{2} (p_q - q')$ | $p_2 = \frac{1}{2} (-k_q + q)$ |

The contributions to the form factors in the impulse approximation are depicted in Fig. 6.1, while the exchange-quark and seagull contributions are shown in Fig. 6.2.

We use $\sigma = \sigma' = 1/2$ in the diquark amplitudes. As discussed in Sec. 2, this implies that the relative momenta p_i within the diquarks are exchange symmetric and that our parameterizations of the diquark BS amplitudes are independent of the mass of the diquark. We thus set,

$$\tilde{\chi}(p_1, k_s) \rightarrow \tilde{\chi}(p_1^2) = \frac{\gamma_5 C}{N_s} P(-p_1^2), \quad (6.16)$$

$$\tilde{\chi}(p_2', p_s) \rightarrow \tilde{\chi}(p_2'^2) = \frac{\gamma_5 C^{-1}}{N_s} P(-p_2'^2).$$

This also simplifies the seagull terms, as the seagull couplings to the diquark legs do not contribute to the seagulls in this case. The amplitudes in the brackets of the last lines of Eqs. (5.31) and (5.32) cancel.

The construction of such vertex functions from the Ward-Takahashi identities is not unique. In particular, the forms for the irreducible seagull couplings M_{sq}^μ and \bar{M}_{sq}^μ given in Eqs. (5.31) and (5.32), respectively, are designed for amplitudes $\tilde{\chi}$ and $\tilde{\chi}$ which are functions of the scalars p_α^2, p_β^2 and, in general, P_d^2 . For $Q \rightarrow 0$, the possibility that the denominators in each of the three terms may vanish entails that the prefactors that arise from expanding the amplitudes in brackets must also vanish.

$$\tilde{\chi}((p_\alpha - Q)^2, p_\beta^2) - \tilde{\chi}(p_\alpha^2, p_\beta^2) \rightarrow -2(p_\alpha Q) \frac{\partial}{\partial p_\alpha^2} \tilde{\chi}(p_\alpha^2, p_\beta^2). \quad (6.17)$$

Our present assumption on the dominant momentum dependence of these amplitudes is slightly different though. For amplitudes $\tilde{\chi} \equiv \tilde{\chi}((p_\alpha - p_\beta)^2/4)$, see (6.16), the prefactors of the seagulls in the form given in Eqs. (5.31)

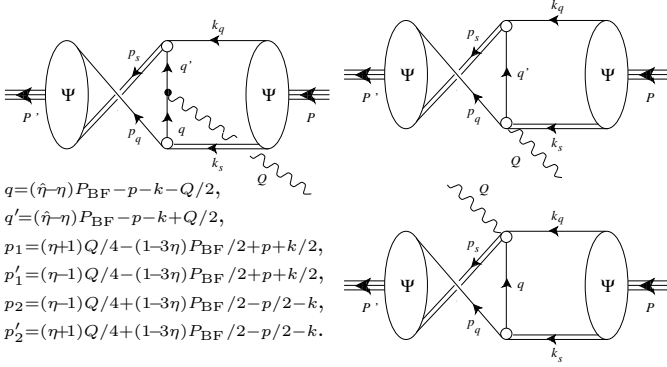


Fig. 6.2. Exchange quark and seagull diagrams.

and (5.32), corresponding to factors $\propto 1/(p_\alpha Q)$ and $\propto 1/(p_\beta Q)$ respectively, are not canceled in an analogous way. To cure this, we replace the quark momenta p_α and p_β in these prefactors by (plus/minus) the relative momentum, $\pm(p_\alpha - p_\beta)/2$. This yields,

$$iM_{sg}^\mu = q_q \frac{(4p'_1 - Q)^\mu}{4p'_1 Q - Q^2} (\tilde{\chi}((p'_1 - Q/2)^2) - \tilde{\chi}(p_1'^2)) \quad (6.18)$$

$$+ q_X \frac{(4p'_1 + Q)^\mu}{4p'_1 Q + Q^2} (\tilde{\chi}((p'_1 + Q/2)^2) - \tilde{\chi}(p_1'^2))$$

$$i\bar{M}_{sg}^\mu = q_q \frac{(4p_2 - Q)^\mu}{4p_2 Q - Q^2} (\tilde{\chi}((p_2 - Q/2)^2) - \tilde{\chi}(p_2^2)) \quad (6.19)$$

$$+ q_X \frac{(4p_2 + Q)^\mu}{4p_2 Q + Q^2} (\tilde{\chi}((p_2 + Q/2)^2) - \tilde{\chi}(p_2^2))$$

Since Ward-Takahashi identities do not completely constrain the form of the vertices, such modification of this type is within the freedom allowed by this ambiguity. The forms (6.18,6.19) solve the corresponding Ward identities at finite Q , see Eq. (5.29) (with $q_q + q_X = q_D$). In addition, the smoothness of the limit $Q \rightarrow 0$ for the given model assumptions is ensured. In this limit,

$$\begin{aligned} iM_{sg}^\mu &\rightarrow -(q_q - q_X) p_1^\mu \tilde{\chi}'(p_1^2), \\ i\bar{M}_{sg}^\mu &\rightarrow -(q_q - q_X) p_2^\mu \tilde{\chi}'(p_2^2). \end{aligned} \quad (6.20)$$

We emphasize that this limit is unambiguous. It must coincide with the form required by the differential form of the Ward identity for the seagull couplings. As such it restricts contributions that are both longitudinal and transverse to the photon four-momentum Q_μ . The form above follows necessarily for the model diquark amplitudes employed in the present study, and this form provides the crucial condition on the seagull couplings that ensure charge conservation for the nucleon bound state.

The nucleon charges are obtained by calculating

$$G_E(0) = \frac{1}{2M} \int \frac{d^4 p}{(2\pi)^4} \frac{d^4 k}{(2\pi)^4} \quad (6.21)$$

$$\text{tr}[\bar{\psi}(-p, P) P_\mu J_{em}^\mu(p, P; k, P) \psi(k, P)].$$

The various contributions to the electromagnetic current for $Q \rightarrow 0$ (i.e., $P' = P$) are given by

$$J_q^\mu \rightarrow i q_q \left(\frac{\partial}{\partial k_q^\mu} S^{-1}(k_q) \right) D^{-1}(k_s) (2\pi)^4 \delta^4(p - k), \quad (6.22)$$

$$J_D^\mu \rightarrow i q_D \left(\frac{\partial}{\partial k_s^\mu} D^{-1}(k_s) \right) S^{-1}(k_q) (2\pi)^4 \delta^4(p - k), \quad (6.23)$$

$$J_X^\mu \rightarrow -i q_X \frac{1}{2N_s^2} P(-p_1^2) P(-p_2^2) \left(\frac{\partial}{\partial q^\mu} S(q) \right), \quad (6.24)$$

$$J_{sg}^\mu \rightarrow i(q_q - q_X) \frac{1}{2N_s^2} S(q) \quad (6.25)$$

$$(p_{1\mu} P'(-p_1^2) P(-p_2^2) - p_{2\mu} P(-p_1^2) P'(-p_2^2)).$$

Comparing this to the normalization integrals given in Sec. 4, one finds

$$G_E(0) = \quad (6.26)$$

$$q_q N_q + q_D N_D + q_X N_X - (q_q - q_X) N_P.$$

Using $q_q = 2/3$, $q_D = 1/3$, $q_X = -1/3$ for the proton, and $q_q = -1/3$, $q_D = 1/3$, $q_X = 2/3$ for the neutron, together with Eq. (4.4), one therefore has,

$$\begin{aligned} 1 &= \eta N_q + (1 - \eta) N_D + (1 - 2\eta) N_X + (1 - 3\eta) N_P, \\ Q_P &= \frac{2}{3} N_q + \frac{1}{3} N_D - \frac{1}{3} N_X - N_P, \\ Q_N &= -\frac{1}{3} N_q + \frac{1}{3} N_D + \frac{2}{3} N_X + N_P. \end{aligned} \quad (6.27)$$

However, these three equations are not independent. Rewriting the normalization condition for the nucleon BS amplitudes, we find that

$$\begin{aligned} 1 &= \frac{2}{3} N_q + \frac{1}{3} N_D - \frac{1}{3} N_X - N_P \\ &\quad + (\eta - \frac{2}{3}) (N_q - N_D - 2N_X - 3N_P), \end{aligned} \quad (6.28)$$

which entails that

$$1 = Q_P + (2 - 3\eta) Q_N. \quad (6.29)$$

To verify that we do in fact obtain the correct charges of the proton and neutron, it suffices to show that $N_q - N_D = 2N_X + 3N_P$; that is, it suffices to show that the neutron is neutral, $Q_N = 0$. The proof of this is straightforward and is given in Appendix C.

6.1 Numerical Computation

The numerical computation of the form factors is done in the Breit frame, where

$$\begin{aligned} Q^\mu &= (0, \mathbf{Q}), \\ P^\mu &= (\omega_Q, -\mathbf{Q}/2), \end{aligned} \quad (6.30)$$

$$P'^\mu = (\omega_Q, \mathbf{Q}/2),$$

$$P_{BF}^\mu = (\omega_Q, 0),$$

$$\text{with } \omega_Q = \sqrt{M^2 + \mathbf{Q}^2/4}.$$

The transformation of these variables to 4-dimensional Euclidean polar coordinates follows the same prescriptions as those employed in Sec. 3 (see Eqs. (3.19)), namely

$$\begin{aligned} \{p^2, k^2, Q^2\} &\rightarrow \{-p^2, -k^2, -Q^2\}, & P_{\text{BF}}^2 &\rightarrow \omega_Q^2, & (6.31) \\ pQ &\rightarrow -p|\mathbf{Q}|y_Q, & kQ &\rightarrow -k|\mathbf{Q}|z_Q, \\ pP_{\text{BF}} &\rightarrow i\omega_Q p y_{\text{BF}}, & kP_{\text{BF}} &\rightarrow i\omega_Q k z_{\text{BF}}, \\ pP' &= pP_{\text{BF}} + pQ/2 \rightarrow \\ & i\omega_Q p y_{\text{BF}} - p|\mathbf{Q}|y_Q/2 =: iM p y, \\ kP &= kP_{\text{BF}} - kQ/2 \rightarrow \\ & i\omega_Q k z_{\text{BF}} + k|\mathbf{Q}|z_Q/2 =: iM k z. \end{aligned}$$

In the presence of two independent external momenta, Q and P_{BF} , we are left with 5 independent angular variables. Together with the absolute values of the integration momenta p and k the exchange-quark and seagull contributions to the form factors at finite momentum transfer Q require performing 7-dimensional integrations. These are computed numerically using Monte Carlo integrations.

For the impulse approximation diagrams, the number of necessary integrations collapses to three due to the momentum-conserving delta functions in Eqs. (6.11) and (6.12). One of the integrations is over the absolute value of the loop momentum k and two are the angular integrations over z_{BF} and z_Q , the cosines of the angles between k and P_{BF} and k and Q , respectively.

The BS amplitudes for the nucleon bound states are given in terms of the two scalar functions $S_1(p, P)$ and $S_2(p, P)$, *c.f.*, Eqs. (3.16) and (3.17) in Sec. 3, which, we recall Eqs. (3.20) and (3.21), are expanded in terms of Chebyshev polynomials T_n to account for their dependence on the azimuthal Euclidean variable,

$$S(p, y) \simeq \sum_{n=0}^{N-1} (-i)^n S_n(p) T_n(y). \quad (6.32)$$

While the argument y of the Chebyshev polynomials, the cosine between relative and total momentum, is in $[-1, 1]$ in the rest-frame of the nucleon, this cannot be simultaneously true for the corresponding arguments in the initial and final nucleon bound-state amplitudes at finite (space-like) momentum transfer Q . In the Breit frame, these arguments are,

$$\begin{aligned} z &= \frac{\omega_Q}{M} z_{\text{BF}} - i \frac{1}{2} \frac{|\mathbf{Q}|}{M} z_Q \quad \text{and} \\ y &= \frac{\omega_Q}{M} y_{\text{BF}} + i \frac{1}{2} \frac{|\mathbf{Q}|}{M} y_Q, \end{aligned} \quad (6.33)$$

for the initial and final nucleon BS amplitudes respectively (with the angular variables z_Q , y_Q and z_{BF} , y_{BF} all in $[-1, 1]$). In order to use the nucleon amplitudes computed from the BSE in the rest frame, analytical continuation into a complex domain is necessary. This can be justified for the bound-state BS wave functions ψ (with legs attached). These can be expressed as vacuum expectation values of local and almost local operators and we can resort to the domain of holomorphy of such expectation values to continue the relative momenta of the bound-state BS wave function $\psi(p, P)$ into the 4-dimensional complex

Euclidean space necessary for the computation of Breit-frame matrix elements from rest-frame nucleon wave functions. The necessary analyticity properties are manifest in the expansion in terms of Chebyshev polynomials with complex arguments.

There are, in general however, singularities associated with the constituent propagators attached to the legs of the bound state amplitudes, here given by the free particle poles on the constituent mass shells. For sufficiently small Q^2 these are outside the complex integration domain. For larger Q^2 , these singularities enter the integration domain. As the general analyticity arguments apply to wave functions ψ rather than the truncated BS amplitudes $\tilde{\psi}$ with 2-component structure $R(p, y)$, it is advantageous to expand these untruncated BS wave functions directly in terms of Chebyshev polynomials (introducing moments $R_n(p)$),

$$R(p, y) \simeq \sum_{n=0}^{N-1} (-i)^n R_n(p) T_n(y), \quad (6.34)$$

and employ the analyticity of Chebyshev polynomials for the BS wave function R . This can be written in terms of the two Lorentz-invariant functions R_1 and R_2 by

$$\begin{aligned} \psi(p, P) &= D(p_s) S(p_q) \tilde{\psi}(p, P) = & (6.35) \\ & D(p_s) S(p_q) \left(S_1(p, P) \Lambda^+(P) + S_2(p, P) \Xi(p, P) \Lambda^+(P) \right) \\ & =: R_1(p, P) \Lambda^+(P) + R_2(p, P) \Xi(p, P) \Lambda^+(P). \end{aligned}$$

The price one must pay, however, is a considerably slower suppression of the higher Chebyshev moments in the expansions in Eq. (6.34) for the BS wave functions compared to the much faster suppression observed for the truncated amplitudes $\tilde{\psi}$. For example, the fourth moments of the truncated nucleon amplitudes $\tilde{\psi}$ are shown in Fig. 3.2 of Sec. 3. Their magnitudes are less than 2 orders of magnitude smaller than the leading Chebyshev moments. However, one must include up to 8 Chebyshev moments in the expansion for the untruncated BS wave functions in order to achieve a comparable reduction.

If the truncated BS amplitudes $\tilde{\psi}$ are used in the expansion, one must account for the singularities of the quark and diquark legs explicitly when these enter the integration domain for some finite values of Q^2 . A naive transformation to the Euclidean metric, such as the one given by Eqs. (6.31), is insufficient. Rather the proper treatment of these singularities is required when they come into the integration domain.

For the impulse-approximate contributions to the form factors we are able to take the corresponding residues into account explicitly in the integration. Although, this is somewhat involved, it is described in Appendix D. For these contributions, one can compare both procedures and verify numerically that they yield the same, unique results, or assess under what conditions they fail to do so.

We have to resort to the BS wave function expansion for calculating the exchange quark and seagull diagrams, however. The residue structure entailed by the structure singularities in the constituent quark and diquark propagators is too complicated in these cases (involving the 7-dimensional integrations). The weaker suppression of the

higher Chebyshev moments and the numerical demands of the multidimensional integrals thus lead to limitations on the accuracy of these contributions at large Q^2 by the available computer resources.

The Dirac algebra necessary to compute G_E and G_M , according to Eqs. (6.8) and (6.9), can be implemented directly into our numerical routines. We use the moments $S_n(p)$ or $R_n(p)$ obtained from the nucleon BSE as described in Sec. 3, which are real scalar functions with positive arguments. These functions are computed on a one-dimensional grid of varying momenta with typically $n_p = 80$ points. Then spline interpolations are used to obtain the values of these functions at intermediate values. The scalar functions $S(p, P)$ and $R(p, P)$ are then easily reconstructed from Eqs. (6.32) and (6.34), respectively. Then complex arguments, as given in Eqs. (6.33), appear in the Chebyshev polynomials when the electromagnetic form factors are calculated.

In the results shown below, the 3-dimensional integrations of the impulse approximation diagrams are performed using Gauss-Legendre or Gauss-Chebyshev quadratures, while the 7-dimensional integrations necessary for the calculation of the exchange-quark and seagull contributions are carried out by means of stochastic Monte-Carlo integrations with 1.5×10^7 grid points. We find that beyond $Q^2 = 3 \text{ GeV}^2$, numerical errors for the stochastic integrations becomes larger than 1% of the numerical result. This we attribute to the continuation of the Chebyshev polynomials $T_n(z)$ to complex values of z as described above.

In addition to the aforementioned complications, there is another bound on the value of Q^2 above which the exchange and seagull diagrams can not be evaluated. It is due to the singularities in the diquark amplitudes $\tilde{\chi}(p_i)$ and in the exchange quark propagator. The rational n -pole forms of the diquark amplitude, $P_{n-P}(p) = (\gamma_n / (\gamma_n + p^2))^n$ for example yield the following upper bound,

$$Q^2 < 4 \left(\frac{4\gamma_n}{(1-3\eta)^2} - M^2 \right). \quad (6.36)$$

A free constituent propagator for the exchange quark gives the additional constraint,

$$Q^2 < 4 \left(\frac{m_q^2}{(1-2\eta)^2} - M^2 \right). \quad (6.37)$$

It turns out, however, that these bounds on Q^2 are insignificant for the model parameters employed in the calculations described herein.

6.2 Results

In Fig. 6.3, we show the electric and magnetic Sachs form factors of the proton and neutron using the parameter sets given in Table 3.1 in Sec. 3 which correspond to a fixed value for the diquark mass $m_s = 0.66 \text{ GeV}$. The nucleon amplitudes used in these calculations correspond to those shown in Fig. 3.4 of Sec. 3. The charge radii obtained by

using the model forms of the diquark BS amplitude given in Table 3.1 are given in Table 6.1.

Examination of the charge radii given in Table 6.1 reveals that the width obtained for the nucleon BS amplitude is closely correlated with the obtained value for the charge radius of the proton. The dipole, quadrupole and exponential forms for the diquark BS amplitude, all give reasonable values for the charge radius of the proton. The accepted value of the proton charge is $r_p \simeq 0.85 \text{ fm}$. However, the width of $S_{1,0}(p)$ does not determine the behavior of the form factors away from $Q^2 = 0$. This is especially clear when the exponential and Gaussian forms are employed for the diquark BS amplitude. In this case, the proton electric form factor ceases to even vaguely resemble the phenomenological dipole fit over most of the range of Q^2 shown in Fig. 6.3. The neutron electric form factor is even more sensitive to the functional form of the diquark amplitudes. The square of charge radius of the neutron depends strongly on the chosen form of the diquark BS amplitude. For the exponential and Gaussian forms, the obtained value of r_n^2 is close to zero, and it is positive when the Gaussian form of the diquark amplitude is used with its peak away from zero (*i.e.*, $x_0 \neq 0$). In Fig. 6.3, we show the form factors that result from using the shifted Gaussian form for the diquark BS amplitude with $x_0/\gamma_{\text{GAU}} = 1$. In fact, the shifted-Gaussian form also produces a node in the electric form factor of the neutron, for which there is no experimental evidence. We conclude that to obtain a realistic description of nucleons, one must rule out the use of forms for the diquark BS amplitude which peak away from the origin.

In Figure 6.4 we compare the $n = 2$ results, obtained from employing the diquark BS amplitude of dipole form, to the experimental data of Refs. [48, 49] and Ref. [50] for the electric form factors of proton and neutron, respectively. In Ref. [50], the neutron G_E is extracted from data taken on an unpolarized deuteron target and with employing various $N-N$ potentials. As pointed out in Ref. [2], due

| | form of diquark amplitude P | r_p (fm) (± 0.02) | r_n^2 (fm ²) (± 0.02) |
|--------------------------|----------------------------------|------------------------------|--|
| fixed $S_{1,0}$ -width : | $n=1$ | 0.78 | -0.17 |
| | $n=2$ | 0.82 | -0.14 |
| | $n=4$ | 0.84 | -0.12 |
| | EXP | 0.83 | -0.04 |
| | GAU | 0.92 | 0.01 |
| | GAU shifted | 1.03 | 0.37 |
| fixed masses: | $n=1$ | 0.97 | -0.24 |
| | $n=2$ | 0.82 | -0.14 |
| | $n=4$ | 0.75 | -0.03 |
| | EXP | 0.73 | -0.01 |

Table 6.1. The electric charge radii for proton and neutron for parameter sets having either the $S_{1,0}$ -width or the quark mass fixed. Error estimates come from the uncertainty in the 7-dimensional integration. The corresponding experimental values are about $r_p \simeq 0.85 \text{ fm}$ for the proton and $r_n^2 \simeq -0.12 \text{ fm}^2$ for the neutron.

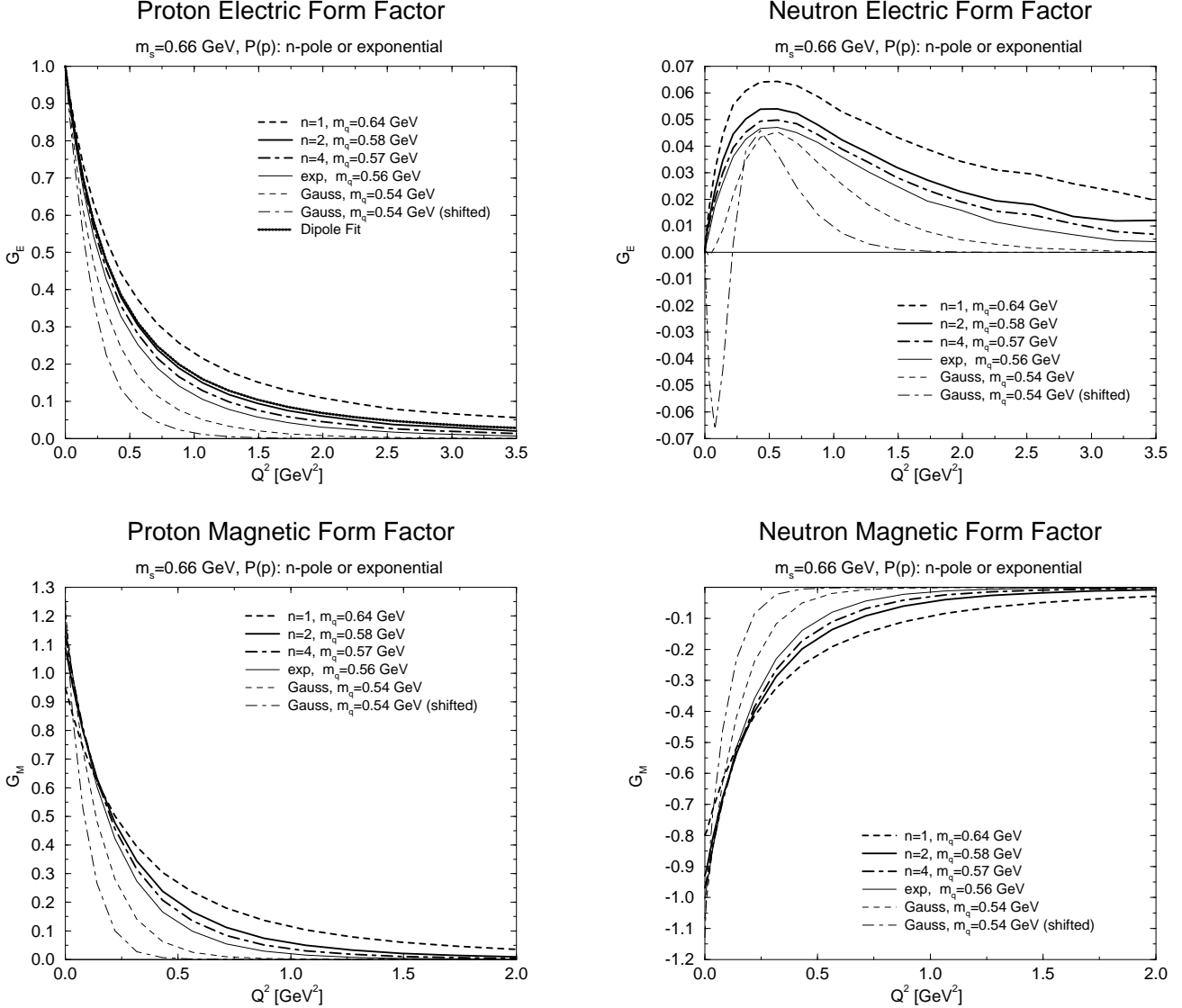


Fig. 6.3. Nucleon electric and magnetic form-factors for fixed widths of $S_{1,0}$. The label Gauss, shifted refers to a calculation with diquark vertex function $P_{\text{GAU}} = \exp(-(p^2/\gamma_{\text{GAU}} - 1)^2)$. The parameters are listed in Tabs. 3.1 and 3.2 in Sec. 3.

to possible systematic errors of this procedure, these results should not be over-interpreted. They can serve to give us a feeling for the qualitative behavior and rough size of the electric form factor of the neutron, however. With resembling the phenomenological dipole fit for the proton fairly well, as seen in Fig. 6.3, it might not be too surprising to discover good agreement also with the experimental results for the proton. However, with the special emphasis of our present study being put on charge conservation, such compelling agreement also for finite photon momentum transfer and over the considerable range of Q^2 (from 0 up to 3.5 GeV^2), seems quite encouraging. Also the neutron electric form factor compares reasonably good with the data, especially considering that we did deliber-

ately not put much effort in adjusting the free parameters in our present model.

The obtained magnetic moments, which range from 0.95 ... 1.26 nuclear magnetons for the proton and from -0.80 ... -1.13 nuclear magnetons for the neutron, are too small. The accepted values for the proton and neutron magnetic moments are 2.79 and -1.91 nuclear magnetons, respectively. The essential reasons for this discrepancy are summarized as follows:

1. The diquark-photon vertex is handled too naively. In this study, we have not included the possibility of an anomalous magnetic moment for the diquark. Using such a simple form, the contributions to the magnetic form factors arise almost exclusively from the quark-photon coupling of the impulse-approximate and ex-

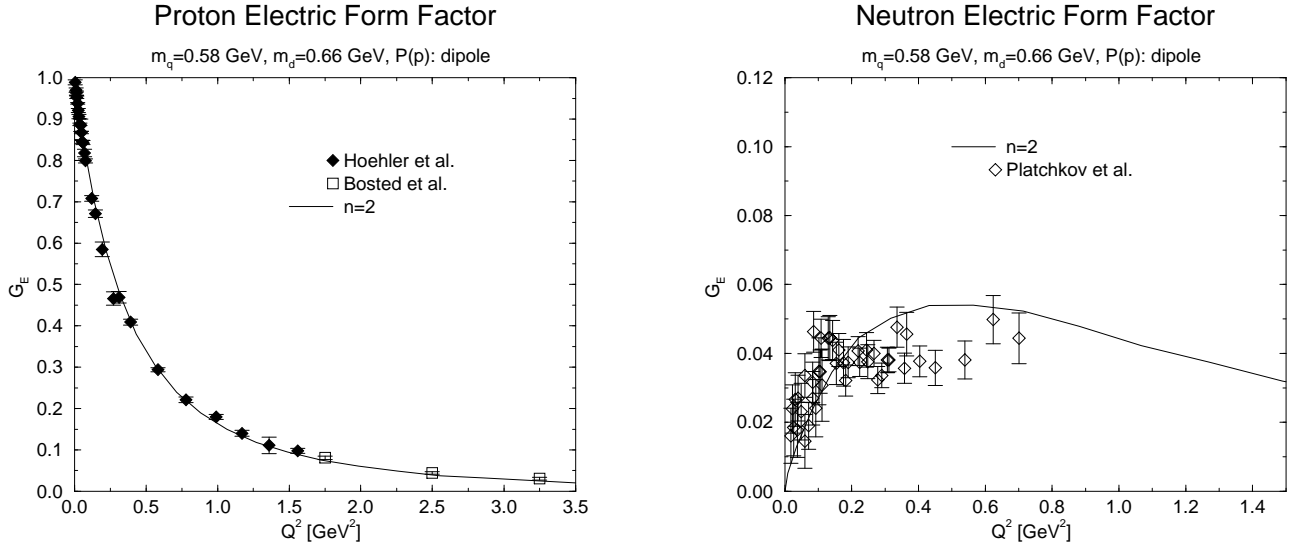


Fig. 6.4. Comparison of the electric form factors of proton and neutron with the experimental data of Refs. [48,49] and Ref. [50], respectively. Here, the dipole form of the diquark amplitude was used corresponding to the $n = 2$ result of Fig. 6.3.

change-quark contributions. A proper resolution of the diquark substructure, by coupling the photon directly to the quarks within the diquark, and taking into account its sub-leading Dirac structure, will lead to an anomalous magnetic moment for the scalar diquark in a natural manner. This was discussed at the end of Sec. 5.1.

2. The consistency requirement is that the strength of the coupling $g_s = 1/N_s$ is given by the normalization of the diquark N_s . At present, this leads to a rather narrow nucleon BS amplitude in combination with somewhat large values for constituent quark mass. Both of these effects tend to suppress the quark contribution to the form factors arising from the impulse-approximate terms. If we had assumed a quark mass m_q of 450 MeV, and artificially increased the width of the diquark BS amplitude, the quark diagram alone would easily contribute 1.3 ... 1.5 nuclear magnetons to the magnetic moment of the proton. That is, a small change to the dynamics of the diquark BS amplitude or mass of the quark can have a significant impact on the magnetic moment of the proton. A similar sensitivity of magnetic moments of vector mesons to the scales in the quark propagator and bound state vector-meson BS amplitude was also observed in Ref. [51].
3. The next important diquark correlation which should be included in a framework like that developed herein is that of the axialvector diquark. The axialvector diquark is necessary for an extension of the quark-diquark model to include a description of the decuplet baryons [36]. It has been observed that the axialvector diquark correlations contribute substantially to the magnetic moments, even at the level of the impulse approximation. This is because even using a pointlike photon-

diquark coupling, one can have currents associated with nucleon spin flips when the axialvector diquark correlation is included. Furthermore, since the axialvector diquark enhances the binding (*i.e.*, lowers the coupling g_s), it tends to lower the quark mass required to produce the same nucleon bound state mass and as discussed above, a smaller quark mass would also serve to improve the obtained values for the magnetic moments.

The electric form factors obtained using the fixed values for quark and diquark masses of $m_q = 0.58$ GeV and $m_s = 0.66$ GeV, respectively, (*i.e.*, for fixed values of the binding energy) are shown in Fig. 6.5. The corresponding charge radii are given in the right half of Table 6.1. The differences between the various diquark amplitude parameterizations considered herein do not lead to such dramatic differing behaviors of the nucleon form factors in this case. Nevertheless, we observed that use of the exponential form of the diquark BS amplitude still produces a proton electric form factor that falls off too fast when compared to the phenomenological dipole fit. It also results in a tiny value for the square of the charge radius of the neutron.

Finally, we compare the relative importance of the various contributions to the form factors that arise from the impulse-approximate, exchange-quark, and seagull diagrams. We separately plot each of these contributions to the total proton and neutron electric form factors in Fig. 6.6 for comparison. For the purposes of comparison, we used the parameter set for the dipole form of the diquark BS amplitude. (This form of the diquark BS amplitude is used because of the excellent description it provides for the the electric form factor of the proton.)

Here, it is interesting to note that the seagull couplings contribute up to about 2/5 of the proton electric form fac-

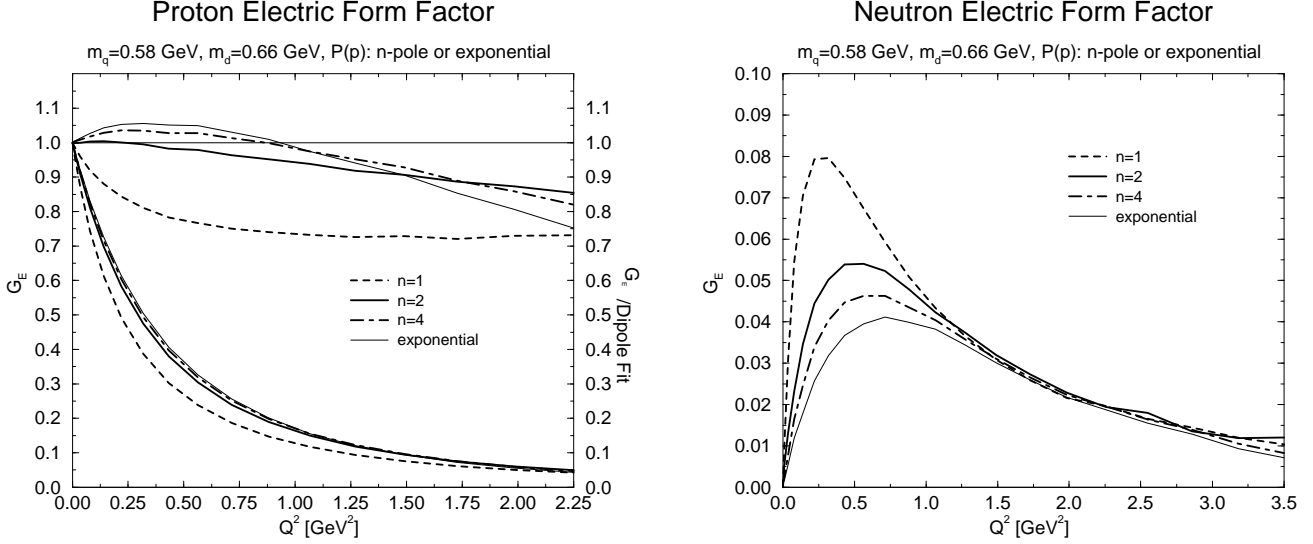


Fig. 6.5. Nucleon electric form factors for fixed quark and diquark masses.

tor $G_E(Q^2)$! It is clear that in the nucleon, these beyond-the-impulse contributions are certainly not negligible. As in the previous discussion of the magnetic moments, where we observed a suppression of the impulse-approximate diagrams arising from the narrow momentum distribution of the nucleon BS amplitude which was a result of employing narrow diquark BS amplitude. Again, we find that employing a diquark BS amplitude that is wider in momentum space leads to a wider nucleon BS amplitude and therefore implies that the impulse approximate contributions are more dominant than the other contributions. This is the case when point-like diquark BS amplitudes are employed, such as in Ref. [35].

For the neutron, we note finally that its electric form factor arises from a sum of large terms which strongly cancel each other to produce a small effect. This cancellation is the explanation for the appearance of “wiggles” in the results for the neutron $G_E(Q^2)$ at moderate Q^2 shown in Figs. 6.3, and 6.5. The wiggles are artifacts of the numerical procedure employed.

7 Conclusions

We have introduced an extension of the covariant quark-diquark model of baryon bound states. The framework developed herein allows for the inclusion of finite-sized diquark correlations in the description of the nucleon bound state in a manner which preserves electromagnetic current conservation for the first time. For such a framework to maintain current conservation of the nucleon, it is necessary to include contributions to the electromagnetic current which arise from the couplings of the photon to the quark-exchange kernel of the nucleon BSE. These contributions are derived from the Ward-Takahashi identities of QED and include the coupling of the photon to the

exchanged quark in the kernel and the photon coupling directly to the BS amplitude of the diquark (the so-called seagull contributions). It was shown analytically that the resulting nucleon current is conserved and these additions are sufficient to ensure the framework provides the correct proton and neutron charges independent of the details of the model parameters.

To explore the utility of this framework under the most simple model assumptions, simple constituent-quark and constituent-diquark propagators and one-parameter model diquark BS amplitudes were employed for the numerical application of the framework. The BS amplitude for the scalar diquark was parametrized by the leading Dirac structure and various forms for the momentum dependence of the amplitude were investigated. It was shown that the antisymmetry of the diquark amplitude under quark exchange places tight constraints on the form of the diquark BS amplitude and that the incorporation of these constraints have the effect of removing much of the model dependence of the diquark BS amplitude parameters from the calculation of the nucleon electromagnetic form factors.

Calculations of the electromagnetic form factors away from $Q^2 = 0$ require that the nucleon BS amplitudes and wave functions be boosted. In this Euclidean-space formulation, this amounts to a continuation of amplitudes and wave functions into complex plane. Two procedures to account for proper handling of poles arising from the constituent particles in the nucleon are described and compared. The feasibility of each procedure is discussed and explored in detail. It is shown analytically and explicitly in a numerical calculation that the two approaches produce the same results for the electromagnetic form factors. Thus, demonstrating that the framework properly accounts for the non-trivial analytic structures of the constituent propagators.

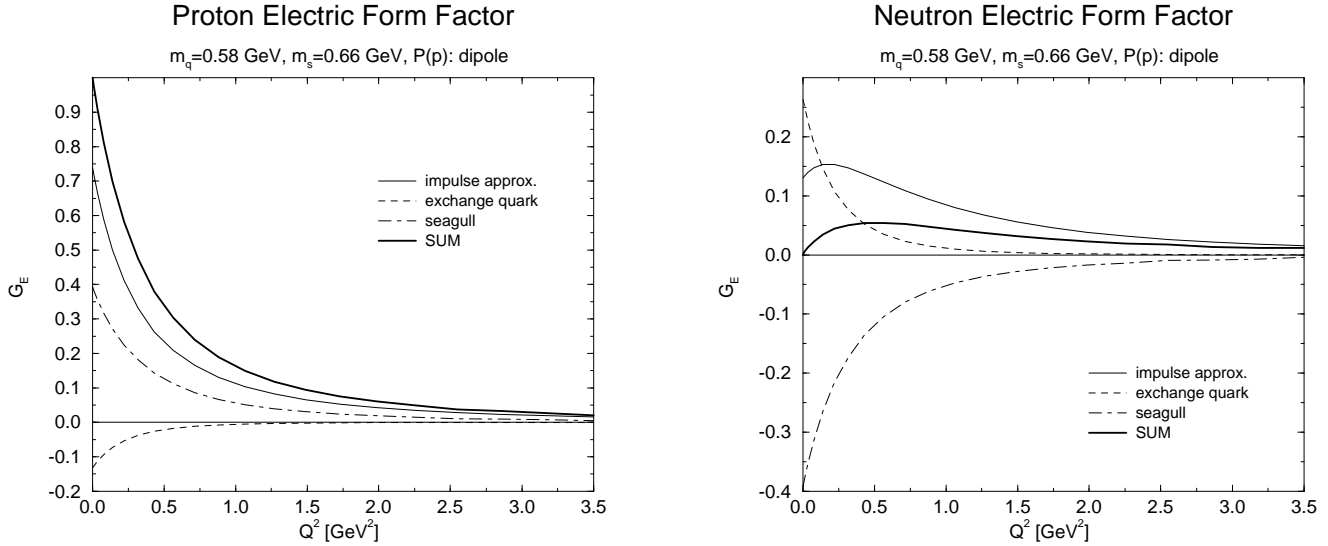


Fig. 6.6. Contribution of the single diagrams to neutron and proton electric form factors. The diquark amplitude is the dipole. The sum of these contributions (SUM) corresponds to the result of Fig. 6.4.

For the particular choice of simple dynamical models explored herein, the masses of the quark and diquark propagators along with the width of the model diquark BS amplitude are the only free parameters in the framework. The latter width is thereby implicitly determined from fixing the nucleon mass. It is shown, for the case of the dipole (and possibly quadrupole) form of the diquark BS amplitude, that these few parameters are sufficient to provide an excellent description of the electric form factors for both the neutron and proton. Other forms of the diquark BS amplitude that were explored, such as the exponential and Gaussian forms, may be ruled out on phenomenological grounds as they lead to nucleon electromagnetic form factors which are inconsistent with the experimental data.

It was found that the framework is at present unable to reproduce the nucleon magnetic moments without the introduction of new parameters such as an anomalous magnetic moment of the diquark. The calculated magnetic moments are smaller than those obtained in experiment by about 50%. Possible explanations for this, including the addition of more complex structures for the scalar diquark correlations, diquark form factors due to their quark substructure which can give rise to anomalous magnetic moments for diquarks, and the effect that the inclusion of other diquark channels (such as the axialvector diquark) would have on the present framework, were discussed. The inclusion of an axialvector diquark within this framework is subject to work currently in progress.

In conclusion, we find that the covariant quark-diquark model of the nucleon provides a framework that is sufficiently rich to describe the electromagnetic properties of the nucleon. However, to ensure that the framework satisfies electromagnetic current conservation one must go beyond the usual impulse approximation diagrams and include contributions that arise from the photon couplings

to the nucleon BSE kernel. In a numerical application of this framework, it was found that these contributions provide a significant part of the electromagnetic form factors of the nucleon and can not be neglected.

Postscript

The necessity of going beyond the impulse approximation when quark-substructure in diquark correlations is taken into account was recently also observed in an exploratory study of the electromagnetic nucleon form factors in Ref. [52]. Therein, a parameterization of the nucleon structure was explored which corresponds to the zeroth Chebyshev moment $S_{1,0}(p)$ of the Lorentz-structure $S_1(p, P)$ in the general nucleon BS amplitude for the bound state of quark and scalar diquark given in Eq. (3.16). Employing a particular parameterization of this simplified nucleon structure the impulse approximation and exchange quark contributions to the form factors were computed in Ref. [52] along with two additional contributions which were necessary for antisymmetrization. The latter two are different from the seagull contributions derived from the Ward identities in our present framework. The antisymmetry on the other hand is manifest in our solution to the nucleon BSE with quark-exchange kernel. Charge conservation was maintained in Ref. [52] for a particular choice of parameters. The normalization constants of diquark and nucleon bound states and the diquark mass parameter were adjusted and the value $\eta = 1/3$ was adopted for the momentum partitioning to ensure the correct charges of the nucleons.

Acknowledgments

The authors gratefully acknowledge valuable discussions with R. Alkofer and N. Ishii.

The work of M.O. was supported by the Deutsche Forschungsgemeinschaft under contract DFG We 1254/4-1. He thanks H. Weigel and H. Reinhardt for their continuing support.

The work of M.A.P. was supported by the U.S. Department of Energy under contracts DE-FG02-87ER40365, DE-AC05-84ER40150 and DE-FG05-92ER40750, the National Science Foundation under contract PHY9722076 and the Florida State University Supercomputer Computations Research Institute which is partially funded by the Department of Energy under contract DE-FC05-85ER25000.

The work of L.v.S. was supported by the U.S. Department of Energy, Nuclear Physics Division, under contract number W-31-109-ENG-38 and by the BMBF under contract number 06-ER-809. Parts of the calculations were performed on the IBM SP3 Quad Machine of the Center for Computational Science and Technology at Argonne National Laboratory.

A Conventions for Diquark Amplitudes

The BS wave functions $\chi(p, P)$ and $\bar{\chi}(p, P)$ of the (scalar) diquark bound-state are defined by the matrix elements,

$$\chi_{\alpha\beta}(x, y; \mathbf{P}) := \langle q_\alpha(x)q_\beta(y) | P_+ \rangle \quad (\text{A.1})$$

$$\begin{aligned} \bar{\chi}_{\alpha\beta}(x, y; \mathbf{P}) &:= \langle P_+ | \bar{q}_\alpha(x)\bar{q}_\beta(y) \rangle, \\ &= (\gamma_0 \chi^\dagger(y, x; \mathbf{P}) \gamma_0)_{\alpha\beta} \end{aligned} \quad (\text{A.2})$$

Note that there is no need for time ordering here in contrast to quark-antiquark bound states. The following normalization of the states is used,

$$\langle P'_\pm | P_\pm \rangle = 2\omega_P (2\pi)^3 \delta^3(\mathbf{P}' - \mathbf{P}), \quad \omega_P^2 = \mathbf{P}^2 + m_s^2, \quad (\text{A.3})$$

and the charge conjugate bound state being $|P_- \rangle = C|P_+ \rangle$. The contribution of the charge conjugate bound state is included in Eq. (2.2) for $P_0 = -\omega_P$. From invariance under space-time translations, the BS wave function has the general form,

$$\chi_{\alpha\beta}(x, y; \mathbf{P}) = e^{-iPX} \int \frac{d^4p}{(2\pi)^4} e^{-ip(x-y)} \chi_{\alpha\beta}(p, P), \quad (\text{A.4})$$

with $X = (1-\sigma)x + \sigma y$, $p := \sigma p_\alpha - (1-\sigma)p_\beta$, and $P = p_\alpha + p_\beta$, where p_α, p_β denote the momenta of the outgoing quarks in the Fourier transform $\chi_{\alpha\beta}(p_\alpha, p_\beta; \mathbf{P})$ of $\chi_{\alpha\beta}(x, y; \mathbf{P})$, see Fig. A.1. One thus has the relation,

$$\chi_{\alpha\beta}(p, P) := \chi_{\alpha\beta}(p + (1-\sigma)P, -p + \sigma P; \mathbf{P}) \Big|_{P_0 = \omega_P}. \quad (\text{A.5})$$

In the definition of the conjugate amplitude, the convention

$$\bar{\chi}_{\alpha\beta}(x, y; \mathbf{P}) = e^{iP\bar{X}} \int \frac{d^4p}{(2\pi)^4} e^{-ip(x-y)} \bar{\chi}_{\alpha\beta}(p, P), \quad (\text{A.6})$$

with $\bar{X} = \sigma x + (1-\sigma)y$, ensures that hermitian conjugation from Eq. (A.2) yields,

$$\bar{\chi}_{\alpha\beta}(p, P) = (\gamma_0 \chi^\dagger(p, P) \gamma_0)_{\alpha\beta}. \quad (\text{A.7})$$

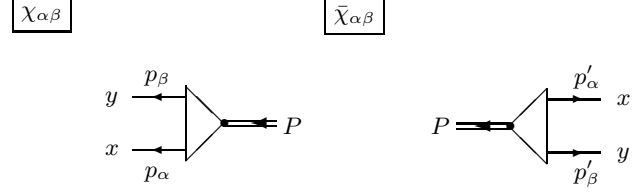


Fig. A.1. The momentum definitions in the diquark amplitudes.

In the conjugate amplitude $\bar{\chi}_{\alpha\beta}(p, P)$, the definition of relative and total momenta corresponds to $p = (1-\sigma)p'_\alpha - \sigma p'_\beta$ and $P = -p'_\alpha - p'_\beta$ for the outgoing quark momenta p'_α, p'_β in

$$\bar{\chi}_{\alpha\beta}(p'_\alpha, p'_\beta; \mathbf{P}) = (\gamma_0 \chi^\dagger(-p'_\beta, -p'_\alpha; \mathbf{P}) \gamma_0)_{\alpha\beta}, \quad (\text{A.8})$$

c.f., Fig. A.1. Note here that hermitian conjugation implies for the momenta of the two respective quark legs, $p_\alpha \rightarrow -p'_\beta$, and $p_\beta \rightarrow -p'_\alpha$, which is equivalent to $\sigma \leftrightarrow (1-\sigma)$ and $P \rightarrow -P$. Besides the hermitian conjugation of Eq. (A.7), one has from the antisymmetry of the wave function, $\chi_{\alpha\beta}(x, y; \mathbf{P}) = -\chi_{\beta\alpha}(y, x; \mathbf{P})$. For the corresponding functions of the relative coordinates/momenta, this entails that σ and $(1-\sigma)$ have to be interchanged in exchanging the quark fields,

$$\chi(x, P) = -\chi^T(-x, P) \Big|_{\sigma \leftrightarrow (1-\sigma)}, \quad (\text{A.9})$$

$$\chi(p, P) = -\chi^T(-p, P) \Big|_{\sigma \leftrightarrow (1-\sigma)}.$$

This interchange of the momentum partitioning can be undone by a charge conjugation, from which the following identity is obtained,

$$\chi^T(p, P) = -C \bar{\chi}(-p, -P) C^{-1}. \quad (\text{A.10})$$

This last identity is useful for relating $\bar{\chi}$ to χ in Euclidean space. In particular, this avoids the somewhat ambiguous definition of the conjugation following from Eq (A.2) in Euclidean space with complex bound-state momenta.

One last definition for diquark amplitudes concerns the truncation of the propagators S attached to the quark legs, thus defining the amputated amplitudes $\tilde{\chi}$ and $\tilde{\bar{\chi}}$ by

$$\chi_{\alpha\beta}(p, P) = (S(p_\alpha) \tilde{\chi}(p, P) S^T(p_\beta))_{\alpha\beta}, \quad (\text{A.11})$$

$$\bar{\chi}_{\alpha\beta}(p, P) = (S^T(-p'_\alpha) \tilde{\bar{\chi}}(p, P) S(-p'_\beta))_{\alpha\beta}. \quad (\text{A.12})$$

With the definitions above, the same relations hold for the amputated amplitudes, in particular,

$$\tilde{\bar{\chi}}(p, P) = \gamma_0 \tilde{\chi}^\dagger(p, P) \gamma_0, \quad (\text{A.13})$$

$$\tilde{\chi}(p, P) = -\tilde{\chi}^T(-p, P) \Big|_{\sigma \leftrightarrow (1-\sigma)}.$$

In Sec. 2 the antisymmetric Green function $G^{(0)}$ for the disconnected propagation of identical quarks with propagator $S(p)$,

$$G_{\alpha\gamma, \beta\delta}^{(0)}(p, q, P) = (2\pi)^4 \delta^4(p - q) \quad (\text{A.14})$$

$$S_{\alpha\beta}(\sigma P - p) S_{\gamma\delta}((1-\sigma)P + p) - \text{crossed term},$$

was used to derive the normalization condition for the diquark amplitudes. This notation is somewhat sloppy. In particular in the second term proportional to $\delta^4(p+q)$, representing the crossed propagation with exchange of the external quark lines, one may use either p or $-q$ in the arguments of the propagators. Exchanging one for the other is possible only with, at the same time, exchanging $\sigma \leftrightarrow 1-\sigma$ as well, however. Momentum conservation entails that incoming and outgoing quark-pairs in successive correlation functions can only be connected if, besides the relative momenta $p = \pm q$, also the momentum partitioning variables of the pairs match. We can include this condition explicitly by introducing temporarily the dimensionless σ' and σ (both in $[0, 1]$) for the incoming and outgoing pair respectively, thus writing,

$$G_{\alpha\gamma,\beta\delta}^{(0)}(p, \sigma, q, \sigma', P) = (2\pi)^4 \delta^4(p-q) \delta(\sigma - \sigma') \quad (\text{A.15})$$

$$S_{\alpha\beta}(\sigma P - p) S_{\gamma\delta}((1-\sigma)P + p)$$

$$- (2\pi)^4 \delta^4(p+q) \delta(\sigma + \sigma' - 1)$$

$$S_{\alpha\delta}(\sigma P - p) S_{\gamma\beta}((1-\sigma)P + p) .$$

The inverse $G^{(0)-1}$ can then be defined as,

$$G_{\alpha\gamma,\beta\delta}^{(0)-1}(p, \sigma, q, \sigma', P) = \frac{1}{4} \left((2\pi)^4 \delta^4(p-q) \delta(\sigma - \sigma') \quad (\text{A.16}) \right.$$

$$S_{\alpha\beta}^{-1}(\sigma P - p) S_{\gamma\delta}^{-1}((1-\sigma)P + p)$$

$$- (2\pi)^4 \delta^4(p+q) \delta(\sigma + \sigma' - 1)$$

$$\left. S_{\alpha\delta}^{-1}(\sigma P - p) S_{\gamma\beta}^{-1}((1-\sigma)P + p) \right) ,$$

giving the exchange antisymmetric unity in the space of (identical) 2-quark correlations upon (left or right) multiplication with $G^{(0)}$,

$$\int \frac{d^4 k}{(2\pi)^4} \int_0^1 d\tilde{\sigma} G_{\alpha\gamma,\rho\omega}^{(0)}(p, \sigma, k, \tilde{\sigma}, P) G_{\rho\omega,\beta\delta}^{(0)-1}(k, \tilde{\sigma}, q, \sigma', P) =$$

$$\frac{1}{2} \left(\delta_{\alpha\beta} \delta_{\gamma\delta} (2\pi)^4 \delta^4(p-q) \delta(\sigma - \sigma') \quad (\text{A.17}) \right.$$

$$\left. - \delta_{\alpha\delta} \delta_{\gamma\beta} (2\pi)^4 \delta^4(p+q) \delta(\sigma + \sigma' - 1) \right) .$$

This is the way the multiplication of 2-quark correlation functions for identical quarks used in Sec. 2 is understood properly. Either Eq. (A.15) or Eq. (A.16) can be used in the derivation of the normalization condition for the diquark amplitude χ for identical quarks, Eq. (2.9).

B Supplements on the Nucleon BSE

In this appendix we would first like to explore the possibility of having exchange-symmetric arguments in the diquark amplitudes of the quark-exchange kernel of the nucleon BSE. Consider the invariant x_1 for the relative momentum in the incoming diquark in the kernel (3.6) corresponding to the definition of the symmetric argument of $P(x)$ given in Eq. (2.12). From Eqs. (3.9) and (3.11) one obtains (with $\sigma + \tilde{\sigma} = 1$ and $\eta + \hat{\eta} = 1$ determining the

momentum partitioning within the diquark and nucleon respectively),

$$x_1 = -p^2 - \sigma \hat{\sigma} k^2 - pk + (1-3\eta)Pp + (2\sigma \hat{\sigma} \hat{\eta} - \eta)Pk$$

$$+ (\eta(1-2\eta) - \sigma \hat{\sigma} \hat{\eta}^2)P^2 . \quad (\text{B.1})$$

One verifies readily that for $\sigma = (1-2\eta)/(1-\eta)$, according to (3.13), the prefactor of the term $\propto P^2$ vanishes, and that of the term $\propto Pk$ becomes $\hat{\sigma}(1-3\eta)$ leaving only the choice $\eta = 1/3$ for a P -independent x_1 . One might now argue that, from the antisymmetry considerations alone, we should be free to add an arbitrary term proportional to the square of the total diquark momentum in the definition of x . We will show now that such a redefinition cannot lead to a P -independent x either (for values of η different from $1/3$). Here, the diquark momentum is $P_D = q + p_\alpha = \hat{\eta}P - k$ and with

$$\hat{x}_1 := x_1 + CP_D^2$$

$$P_D^2 = \hat{\eta}^2 P^2 - 2\hat{\eta}Pk + k^2 , \quad (\text{B.2})$$

one finds that in order to have no terms $\propto P^2$ in \hat{x}_1 ,

$$C = -\hat{\eta}^{-2}(\eta(1-2\eta) - \sigma \hat{\sigma} \hat{\eta}^2) . \quad (\text{B.3})$$

With this C , however, one has

$$\hat{x}_1 = -p^2 - \eta \hat{\eta}^{-2}(1-2\eta)k^2 - pk + (1-3\eta)(Pp + \eta \hat{\eta}^{-1}Pk) ,$$

independent of σ . This shows that the symmetric arguments of the diquark amplitudes χ and, analogously, $\bar{\chi}$ can quite generally be independent of the total nucleon momentum P only for $\eta = 1/3$.

The remainder of this appendix describes the structure of the nucleon BSE for the bound-state of scalar diquark and quark in some more detail. The form of the bound-state pole in the scalar-fermion 4-point function, Eq. (3.1), implies that the corresponding bound-state amplitudes obey,

$$\tilde{\psi}(p, P_n) \Lambda^+(P_n) = \tilde{\psi}(p, P_n) , \quad (\text{B.4})$$

$$\Lambda^+(P_n) \tilde{\bar{\psi}}(p, P_n) = \tilde{\bar{\psi}}(p, P_n) ,$$

with $\Lambda^+(P_n) = (\not{P}_n + M_n)/2M_n$. Therefore, the amplitudes can be decomposed as follows:

$$\tilde{\psi}(p, P_n) = \quad (\text{B.5})$$

$$S_1(p, P_n) \Lambda^+(P_n) + S_2(p, P_n) \Xi(p, P_n) \Lambda^+(P_n) ,$$

$$\tilde{\bar{\psi}}(p, P_n) = \quad (\text{B.6})$$

$$S_1(-p, P_n) \Lambda^+(P_n) + S_2(-p, P_n) \Lambda^+(P_n) \Xi(-p, P_n) ,$$

with $\Xi(p, P_n) = (\not{p} - pP_n/M_n)/M_n$. This simply separates positive from negative energy components of the amplitudes,

$$\not{P}_n \Lambda^+(P_n) = M_n \Lambda^+(P_n) , \quad (\text{B.7})$$

$$\not{P}_n \Xi(p, P_n) \Lambda^+(P_n) = -M_n \Xi(p, P_n) \Lambda^+(P_n) ,$$

$$\text{and thus, } \Lambda^+(P_n) \Xi(p, P_n) \Lambda^+(P_n) = 0 .$$

One furthermore has,

$$\Lambda^+(P_n) \Xi(p, P_n) \Xi(p, P_n) \Lambda^+(P_n) = \quad (\text{B.8})$$

$$\left(\frac{p^2}{M_n^2} - \frac{(pP_n)^2}{M_n^4} \right) \Lambda^+(P) ,$$

which allows to rewrite the homogeneous BSE (3.4) in terms of 2-vectors $S^T(p, P_n) := (S_1(p, P_n), S_2(p, P_n))$, using the kernel (3.6),

$$S(p, P_n) = \frac{1}{2N_s^2} \int \frac{d^4k}{(2\pi)^4} P(x_1)P(x_2) D(k_s) T(p, k, P_n) S(k, P_n), \quad (\text{B.9})$$

with $k_s = (1-\eta)P_n - k$, $k_q = k + \eta P_n$ and

$$T(p, k, P_n) = \frac{1}{2} \begin{pmatrix} 1 & 0 \\ 0 & \left(\frac{p^2}{M_n^2} - \frac{(pP_n)^2}{M_n^4} \right)^{-1} \end{pmatrix} \times \quad (\text{B.10})$$

$$\begin{pmatrix} \text{tr} \{ S(q) S(k_q) \Lambda^+(P_n) \} \\ \text{tr} \{ S(q) S(k_q) \Lambda^+(P_n) \Xi(p, P_n) \} \\ \text{tr} \{ S(q) S(k_q) \Xi(k, P_n) \Lambda^+(P_n) \} \\ \text{tr} \{ S(q) S(k_q) \Xi(k, P_n) \Lambda^+(P_n) \Xi(p, P_n) \} \end{pmatrix}.$$

After performing these traces the transfer to Euclidean metric introducing 4-dimensional polar variables is done according to the prescriptions,

$$\begin{aligned} p^2, k^2 &\rightarrow -p^2, -k^2, & P_n^2 &\rightarrow M_n^2, \\ pP_n &\rightarrow iM_n p y, & kP_n &\rightarrow iM_n k z, \\ pk &\rightarrow -k p u(x, y, z), \\ u(x, y, z) &= yz + x \sqrt{1-y^2} \sqrt{1-z^2}. \end{aligned} \quad (\text{B.11})$$

In these variables, the nucleon BS-amplitudes are functions of the modulus of the relative momentum and its azimuthal angle with the total momentum. The matrix T in the kernel, in addition to the moduli p, k and azimuthal angles y, z of both relative momenta, also depends on the angle u between them,

$$\begin{aligned} S(p, P_n) &\rightarrow S(p, y), \\ T(p, k, P_n) &\rightarrow T(p, y, k, z, u(x, y, z)). \end{aligned} \quad (\text{B.12})$$

The azimuthal dependence of the amplitudes is taken into account by means of a Chebyshev expansion to order N , see, e.g., Ref. [53],

$$S(p, y) \simeq \sum_{n=0}^{N-1} (-i)^n S_n(p) T_n(y), \quad (\text{B.13})$$

$$S_n(p) = i^n \frac{2}{N} \sum_{k=1}^N S(p, y_k) T_n(y_k), \quad (\text{B.14})$$

where the $y_k = \cos\left(\frac{\pi(k-1/2)}{N}\right)$

are the zeros of the Chebyshev polynomial of degree N . Here, Chebyshev polynomials of the 1st kind are used with, for later convenience, a somewhat non-standard normalization $T_0 := 1/\sqrt{2}$. An explicit factor $(-i)^n$ was introduced in order to obtain real Chebyshev moments $S_n(p)$ for all n . Analogous formulae are obtained for expansions in Chebyshev polynomials of the 2nd kind, which are used in Refs. [35,36]. The nucleon BSE now reads,

$$S_m(p) = -\frac{1}{2N_s^2} \int \frac{k^3 dk}{(4\pi)^2} \sum_{n=0}^{N-1} i^{m-n} T_{mn}(p, k) S_n(k), \quad (\text{B.15})$$

with

$$T_{mn}(p, k) = \frac{2}{\pi} \int_{-1}^1 \sqrt{1-z^2} dz \quad (\text{B.16})$$

$$\frac{1}{x_s + m_s^2} \int_{-1}^1 dx \frac{2}{N} \sum_{k=1}^N \left(P(x_1) P(x_2) \right)_{y=y_k}$$

$$T(p, y_k, k, z, u(x, y_k, z)) T_m(y_k) T_n(z),$$

where $x_s = k^2 + 2i(1-\eta)M_n k z - (1-\eta)^2 M_n^2$ is the invariant momentum of the free scalar propagator D of mass m_s .

C Supplements on Nucleon Charge Conservation

The missing step in the explicit verification of the correct charges $Q_P = 1$ for the proton and $Q_N = 0$ for the neutron is to prove that

$$N_q - N_D = 2N_X + 3N_P \quad (\text{C.1})$$

which is equivalent to $Q_N = 0$, see Eqs. (6.27) to (6.29) in Sec. 6. To this end, note that from Eqs. (4.5) and (4.6) the l.h.s above can be written as,

$$N_q - N_D = \frac{P^\mu}{2M_n} i \int \frac{d^4k}{(2\pi)^4} \quad (\text{C.2})$$

$$\text{tr} \left[\bar{\psi}(-k, P) \left(\frac{\partial}{\partial k^\mu} S^{-1}(k_q) D^{-1}(k_s) \right) \psi(k, P) \right]$$

$$= \frac{P^\mu}{2M_n} i \int \frac{d^4k}{(2\pi)^4}$$

$$\text{tr} \left[\bar{\psi}(-k, P) \left(\frac{\partial}{\partial k^\mu} S^{-1}(k_q) D^{-1}(k_s) \psi(k, P) \right) \right]$$

$$+ \left(\frac{\partial}{\partial k^\mu} \bar{\psi}(-k, P) S^{-1}(k_q) D^{-1}(k_s) \right) \psi(k, P) \right]$$

– total derivative ,

with $k_q = \eta P + k$ and $k_s = \hat{\eta} P - k$ as in the previous sections. A surface term which vanishes for normalizable BS wave functions ψ and $\bar{\psi}$ was not given explicitly. Using the BSEs for $\tilde{\psi} = S^{-1} D^{-1} \psi$ and $\tilde{\bar{\psi}} = \bar{\psi} S^{-1} D^{-1}$, c.f., Eqs. (5.7) and (5.8), in analogy to the proof of current conservation in Sec. 5, one obtains,

$$N_q - N_D = \frac{P^\mu}{2M_n} i \int \frac{d^4p}{(2\pi)^4} \frac{d^4k}{(2\pi)^4} \quad (\text{C.3})$$

$$\text{tr} \left[\bar{\psi}(-p, P) \left(\frac{\partial}{\partial p^\mu} K(p, k, P) + \frac{\partial}{\partial k^\mu} K(p, k, P) \right) \psi(k, P) \right].$$

From Eq. (3.6) for the explicit form of the exchange kernel it follows that

$$\left(\frac{\partial}{\partial p^\mu} + \frac{\partial}{\partial k^\mu} \right) K(p, k, P) = -\frac{1}{2N_s^2} \quad (\text{C.4})$$

$$\left\{ 2 \left(\frac{\partial}{\partial q^\mu} S(q) \right) P(-p_1^2) P(-p_2^2) + S(q) \left(3p_{1\mu} P_1'(-p_1^2) P(-p_2^2) - 3p_{2\mu} P_1(-p_1^2) P'(-p_2^2) \right) \right\},$$

$$\begin{array}{ccc}
\int \bar{\psi}_M D_M^{-1} \Gamma_{q,M}^\mu \psi_M & \xrightarrow{\text{Wick rotation}} & \int \bar{\psi}_E D_E^{-1} \Gamma_{q,E}^\mu \psi_E \\
\tilde{\psi}_M = S_M^{-1} D_M^{-1} \psi_M \downarrow & & \downarrow \tilde{\psi}_E \neq S_E^{-1} D_E^{-1} \psi_E \\
\int \tilde{\psi}_M S_M \Gamma_{q,M}^\mu S_M D_M \tilde{\psi}_M & \xrightarrow{\text{Wick rotation}} & \int \tilde{\psi}_E S_E \Gamma_{q,E}^\mu S_E D_E \tilde{\psi}_E \\
& & + \text{residue terms}
\end{array}$$

Fig. C.1. Interrelation of matrix elements in Minkowski and Euclidean space. The integral sign is shorthand for the four-dimensional integration over the relative momentum k , see Eq. (D.1).

since $q = (1-2\eta)P - p - k$, $p_1 = -(1-3\eta)P/2 + p + k/2$ and $p_2 = (1-3\eta)P/2 - p/2 - k$. Comparing to the definitions of N_X and N_P , Eqs. (4.7) and (4.8) in Sec. 4 respectively, we see that Eq. (C.4) inserted in Eq. (C.3) gives (C.1) as required.

D Calculation of the Impulse Approximation Diagrams

In this appendix we discuss the difficulties in the formal transition from the Minkowski to the Euclidean metric which are encountered in the connection between Bethe-Salpeter amplitudes $\tilde{\psi}$ and Bethe-Salpeter wave functions ψ in a general (boosted) frame of reference of the nucleon bound state.

As the generic example for this discussion, we choose the first diagram in Figure 6.1 which describes the impulse-approximate contribution arising from the coupling of the photon to the quark within the nucleon, $\langle \hat{J}_q^\mu \rangle$ according to Eq. (6.10) with Eq. (6.11). Please refer to Fig. 6.1 and Table 6.15 for the momentum definitions employed herein.

In the Mandelstam formalism, such matrix elements between bound states are related to the corresponding BS wave functions in the Minkowski space, here to the nucleon BS wave functions ψ_M .² Upon the transition to the Euclidean metric, the corresponding contribution to the observable, here to the nucleon form factors, is determined by the ‘‘Euclidean BS wave function’’ ψ_E . In the rest frame of the nucleon bound state this transfer from $M \rightarrow E$ of the BS wave functions commutes with the replacement of the wave functions by the truncated BS amplitudes; that is, unique results are obtained from the Euclidean contributions based on either employing the Minkowski space wave functions or the BS amplitudes which are related by the truncation of the propagators of the constituent legs, here $\tilde{\psi}_M = S_M^{-1} D_M^{-1} \psi_M$, or, *vice versa*, $\psi_M = S_M D_M \tilde{\psi}_M$.

At finite momentum transfer Q^2 one needs to employ BS wave functions in a more general frame of reference, here we use the Breit frame in which neither the incoming nor the outgoing nucleon are at rest. As described in Sec. 6, the ‘‘Euclidean wave function’’ ψ_E in this frame is obtained from the solution to the BSE in the rest frame by

analytic continuation, in particular, by inserting complex values for the argument of the Chebyshev polynomials, see Eqs. (6.33). This corresponds to the transition from left to right indicated by the arrow of the upper line in Figure C.1.

In the analogous transition on the other hand, when the truncated BS amplitudes are employed, the possible presence of singularities in the propagators of legs has to be taken into account explicitly. In the present example, these are the simple particle poles of the propagators of the constituent quark and diquark that might be encircled by the closed path in the k_0 -integration. The corresponding residues have to be included in the transition to the Euclidean metric in this case, which is indicated in the lower line of Fig. C.1.

The conclusion is therefore that the naive relation between BS amplitudes and wave functions can not be maintained in the Chebyshev expansion of the Euclidean spherical momentum coordinates when singularities are encountered in the truncation of the legs. Resorting to the Minkowski space definitions of BS amplitudes vs. wave functions, however, unique results are obtained from either employing the domain of holomorphy of the BS wave functions in the continuation to the Euclidean metric (with complex momenta) or, alternatively and technically more involved, from keeping track of the singularities that can occur in the Wick rotation when the truncated amplitudes and explicit constituent propagators are employed.

The rest of this section concerns the description of how to account for these singularities which, for our present calculations employing constituent poles for quark and diquark, give rise to residue terms as indicated in the lower right corner of Fig. C.1.

To this end consider the quark contribution to the matrix elements of the electromagnetic current which, from Eq. (6.10) with Eq. (6.11), is given by

$$\begin{aligned}
\langle \hat{J}_q^\mu \rangle &= q_q \int \frac{d^4 k}{(2\pi)^4} \\
&\tilde{\psi}(-k - \hat{\eta}Q, P') D(k_s) S(p_q) \Gamma_{quark}^\mu S(k_q) \tilde{\psi}(k, P).
\end{aligned} \tag{D.1}$$

We are interested in the location of the propagator poles herein. For these poles, solving the corresponding quadratic equation for the zeroth component of the relative momen-

² In the following the subscript M stands for definitions in Minkowski space and E for the corresponding ones in Euclidean space.

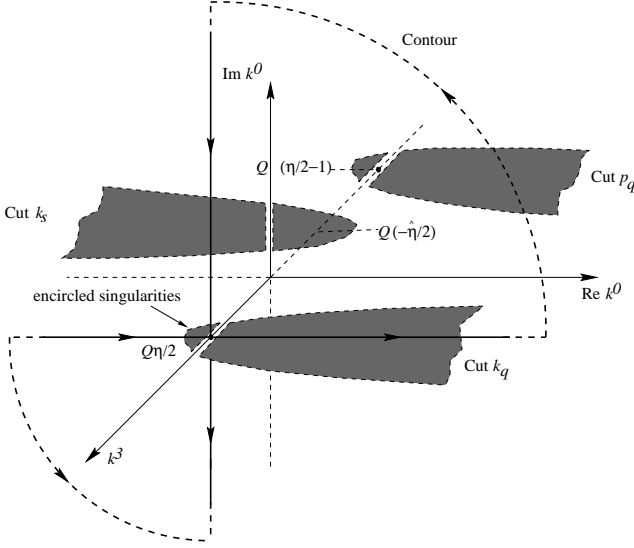


Fig. D.1. Location of the relevant singularities in the impulse-approximate quark contribution to the form factors. The relative momentum k is the integration variable in the loop diagram corresponding to Eq. (D.1).

tum k^0 , from Table 6.15 and Eqs. (6.30), yields

$$k_q^2 - m_q^2 - i\epsilon = 0 \Leftrightarrow \quad (\text{D.2})$$

$$k_{pole,1}^0 = -\eta\omega_Q \pm W(m_q, (\mathbf{k} - \eta/2 \mathbf{Q})^2)$$

$$p_q^2 - m_q^2 - i\epsilon = 0 \Leftrightarrow \quad (\text{D.3})$$

$$k_{pole,2}^0 = -\eta\omega_Q \pm W(m_q, (\mathbf{k} - (\eta/2 - 1)\mathbf{Q})^2)$$

$$k_s^2 - m_s^2 - i\epsilon = 0 \Leftrightarrow \quad (\text{D.4})$$

$$k_{pole,3}^0 = \hat{\eta}\omega_Q \pm W(m_s, (\mathbf{k} + \hat{\eta}/2 \mathbf{Q})^2)$$

with $W(m, \mathbf{k}^2) = \sqrt{\mathbf{k}^2 + m^2 - i\epsilon}$ (and $\eta + \hat{\eta} = 1$).

For $Q = 0$, *i.e.*, in the rest frame of the nucleon in which the Bethe-Salpeter equation was solved, the naive Wick rotation is justified for $1 - \frac{m_s}{M} < \eta < \frac{m_q}{M}$, since there always is a finite gap between the cuts contained in the hypersurface $\text{Re}k^0 = 0$ of the $\text{Re}k^0 - \text{Im}k^0 - \mathbf{k}$ space. As Q increases, these cuts begin to be shifted along both, the k^3 and the k^0 -axis, as sketched in Figure D.1. This eventually amounts to the effect that one of the two cuts arising from each propagator crosses the $\text{Im}k^0$ -axis. As indicated in the figure, Wick rotation $k^0 \rightarrow ik^4$ is no longer possible for arbitrary values of k^3 without encircling singularities. The corresponding residues thus lead to

$$\langle \hat{J}_q^\mu \rangle \rightarrow q_q \int_E \frac{d^4k}{(2\pi)^4} \quad (\text{D.5})$$

$$\tilde{\psi}(-\mathbf{k} - \hat{\eta}\mathbf{Q}, P') D(k_s) S(p_q) \Gamma_q^\mu S(k_q) \tilde{\psi}(\mathbf{k}, P)$$

$$+ i \int \frac{d^3\mathbf{k}}{(2\pi)^3} \theta_{\mathbf{k}} \tilde{\psi}(-k_{pole,1}^4, -\mathbf{k} - \hat{\eta}\mathbf{Q}, P') D(k_s) S(p_q) \times$$

$$\Gamma_q^\mu \text{Res}(S(k_q)) \psi(k_{pole,1}^4, \mathbf{k}, P)$$

$$+ \text{analogous terms for } S(p_q) \text{ and } D(k_s)$$

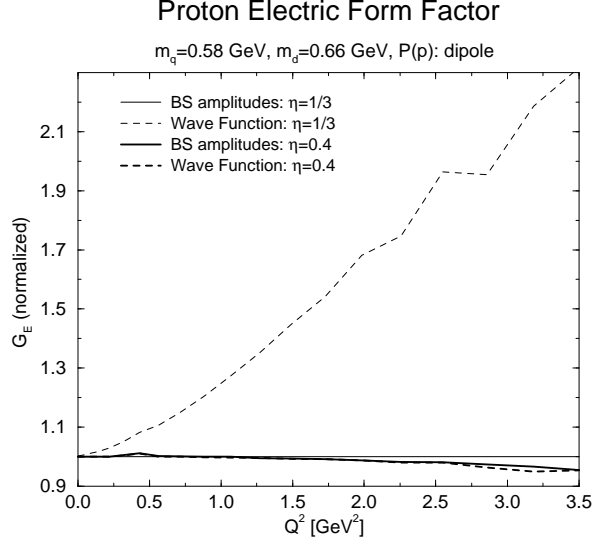


Fig. D.2. The impulse-approximate contribution, corresponding to the diagrams of Fig. 6.1, to the electric form factor of the proton (employing the dipole diquark amplitude). Results of the BS wave function calculations for the η -values 1/3 and 0.4 are compared to the respective amplitude plus residue calculations. The results are normalized to the latter with $\eta=1/3$.

upon transforming Eq. (D.1) to the Euclidean metric. Here, the residue integral is evaluated at the position of the pole in the incoming quark propagator $S(k_q)$ on the Euclidean k^4 -axis

$$k_{pole,1}^4 = -i\eta\sqrt{M^2 + Q^2/4} + iW(m_q, (\mathbf{k} - \eta/2 \mathbf{Q})^2),$$

where $\text{Res}(S(k_q))$ denotes the corresponding residue, and the abbreviation

$$\theta_{\mathbf{k}} \equiv \theta(\eta\omega_Q - W(m_q, (\mathbf{k} - \eta/2 \mathbf{Q})^2))$$

was adopted to determine the integration domain for which the encircled singularities of Figure D.1 contribute.

Analogous integrals over the spatial components of the relative momentum \mathbf{k} arise from the residues corresponding to the poles in the outgoing quark propagator $S(p_q)$ and the diquark propagator $D(k_s)$ as given in Eqs. (D.3) and (D.4).

One verifies that these cuts (as represented by the shaded areas in Fig. D.1) never overlap. Pinching of the deformed contour does not occur, since there are no anomalous thresholds for spacelike momentum transfer Q^2 in these diagrams.

In Figure D.2 we compare results for the electric form factor of the proton employing the nucleon BS amplitudes, together with the procedure to account for the singularities as outlined above, with the corresponding wave function calculations. The $n = 2$ dipole diquark amplitude of Sec. 3 is employed herein once more. For $\eta = 1/3$ the Chebyshev expansion of the BS wave function to 9 orders still turns out insufficient to provide for stable numerical results. This is due to being too close to the range in η that requires proper treatment of the diquark pole contribution

to the nucleon BSE which, with the present value of the mass $m_s/M = 0.7$ is the case for $\eta \leq 1 - m_s/M = 0.3$. The considerably weaker suppression of higher orders in the Chebyshev expansion of the BS wave function as compared to the expansion of the BS amplitude enhances the residual η -dependence of the observables obtained from the former expansion at a given order, in particular, when it has to reproduce close-by pole contributions in the constituent propagators. The impulse-approximate contributions to G_E deviate substantially from those employing the BS amplitude and residue calculations in this case. On the other hand, for values of the momentum partitioning variable which are a little larger than $1/3$ such as $\eta = 0.4$ used in the other results of Fig. D.2, unique results are obtained from both procedures. Both, the BS wave function and amplitude calculation are in perfect agreement for values of the momentum partitioning that are closer to the middle of the range allowed to η .

For the seagull and exchange quark contributions corresponding to the diagrams of Fig. 6.2 an analogous anal-

ysis of the singularity structure is considerably more complicated. The explicit inclusion of their contributions which allowed the calculation based on the BS amplitude expansion also of these diagrams is numerically too involved. For these contributions to the form factors we have to resort to the BS wave function calculations. Unlike the impulse-approximate contributions we find, however, that the deviations in the results for the exchange quark and seagull contributions for $\eta = 1/3$ and $\eta = 0.4$ are smaller than the numerical accuracy of the calculations and thus negligible. We attribute this to the fact that the exchange quark and seagull contributions to the form factors tend to fall off considerably faster with increasing Q^2 than those of the impulse approximation. This can be seen in Figure 6.6.

Small residual η -dependences are observed for the momentum transfers above 3GeV^2 also in the otherwise stable calculations. These give rise to deviations in the results for the form factors of at most 4% which decrease rapidly and become negligible at lower Q^2 .

References

1. M. Ostrick *et al.*, Phys. Rev. Lett. **83** (1999), 276.
2. I. Passchier *et al.*, Phys. Rev. Lett. **82** (1999), 4988; D. J. Boersma, *for the 9405 Collaboration*, e-print, nucl-ex/9908003.
3. M. Gell-Mann, Phys. Rev. **8** (1964), 214.
4. G. Karl and E. Obryk, Nucl. Phys. B **8** (1968), 609.
5. D. Faiman and A. W. Hendry, Phys. Rev. **173** (1968), 1720.
6. R. P. Feynman, M. Kislinger and F. Ravndal, Phys. Rev. D **3** (1971), 2706.
7. A. Chodos, R. L. Jaffe, K. Johnson, C. Thorn and V. F. Weisskopf, Phys. Rev. D **9** (1974), 3471; A. Chodos, R. L. Jaffe, K. Johnson and C. Thorn, Phys. Rev. D **10** (1974), 2599.
8. P. Hasenfratz and J. Kuti, Phys. Rep. **40** (1978), 75.
9. T. H. R. Skyrme, Proc. R. Soc. **127** (1961), 260.
10. G. S. Adkins, C. R. Nappi and E. Witten, Nucl. Phys. B **228** (1983), 552.
11. B. Schwesinger, H. Weigel, G. Holzwarth and A. Hayashi, Phys. Rep. **173** (1989), 173.
12. G. Holzwarth (Ed.), *Baryons as Skyrme Solitons*, World Scientific, Singapore, 1993.
13. R. Alkofer, H. Reinhardt and H. Weigel, Phys. Rep. **265** (1996), 139.
14. C. V. Christov et al, Prog. Part. Nucl. Phys. **37** (1996), 1.
15. H. Reinhard, Phys. Lett. B **244** (1990), 316.
16. A. Buck, R. Alkofer, and H. Reinhardt, Phys. Lett. B **286** (1992), 29.
17. N. Ishii, W. Bentz and K. Yazaki, Phys. Lett. B **301** (1993), 165; Phys. Lett. B **318** (1993), 26; Nucl. Phys. A **587** (1995), 617.
18. S. Huang and J. Tjon, Phys. Rev. C **49** (1994), 1702.
19. A. Buck, and H. Reinhardt, Phys. Lett. B **356** (1995), 168.
20. H. Asami, N. Ishii, W. Bentz and K. Yazaki, Phys. Rev. C **51** (1995), 3388.
21. R. T. Cahill Aust. J. Phys. **42** (1989), 171.
22. C. J. Burden, R. T. Cahill and J. Praschifka, Aust. J. Phys. **42** (1989), 147.
23. A. Chodos and C. Thorn, Phys. Rev. D **12** (1975), 2733.
24. M. Rho, Phys. Rep. **240** (1994), 1.
25. U. Zückert, R. Alkofer, H. Weigel and H. Reinhardt, Phys. Rev. C **55** (1997), 2030; see also, U. Zückert, *Baryonen als Hybride: Chirale Solitonen und gebundene Drei-quarkzustände*, Dissertation, Tübingen University, 1996.
26. L. von Smekal, A. Hauck, and R. Alkofer, Phys. Rev. Lett. **79** (1997), 3591.
27. L. von Smekal, A. Hauck, and R. Alkofer, Ann. Phys. **267** (1998), 1.
28. C. J. Burden, C. D. Roberts and M. J. Thomson, Phys. Lett. B **371**, 163.
29. C. D. Roberts, Nucl. Phys. A **605** (1996), 475.
30. M. A. Pichowsky and T.-S.H. Lee, Phys. Rev. D **56** (1997), 1644.
31. V. A. Miransky, “Dynamical Symmetry Breaking in Quantum Field Theories”, World Scientific, 1993, and references therein.
32. C. D. Roberts and A. G. Williams, Prog. Part. Nucl. Phys. **33** (1994), 477.
33. P. C. Tandy, Prog. Part. Nucl. Phys. **39** (1997), 117.
34. K. Kusaka, G. Piller, A. W. Thomas, and A. G. Williams, Phys. Rev. D **55** (1997), 5299.
35. G. Hellstern, R. Alkofer, M. Oettel and H. Reinhardt, Nucl. Phys. A **627** (1997), 679.
36. M. Oettel, G. Hellstern, R. Alkofer and H. Reinhardt, Phys. Rev. C **58** (1998), 2459.
37. J. Praschifka, R. T. Cahill and C. D. Roberts, Int. J. Mod. Phys. A **4** (1989), 4929.
38. A. Bender, C. D. Roberts and L. v. Smekal, Phys. Lett. B **380** (1996), 7.
39. G. Hellstern, R. Alkofer and H. Reinhardt, Nucl. Phys. A **625** (1997), 697.
40. R. Oehme, Int. J. Mod. Phys. A **10** (1995), 1995.
41. J. Praschifka, R. T. Cahill and C. D. Roberts, Mod. Phys. Lett. A **3** (1988), 1595.
42. S. Mandelstam, Proc. Roy. Soc. **233** A (1955), 248.
43. K. Otha, Phys. Rev. C **40** (1989), 1335.
44. S. Wang and M. K. Banerjee, Phys. Rev. C **54** (1996), 2883.
45. F. Gross and D. O. Riska, Phys. Rev. C **36** (1987), 1928.
46. R. Peierls, *The Commutation Laws of Relativistic Quantum Field Theory*, Proc. Roy. Soc. A **214** (1952), 143; see also, Sec. I.4 in R. Haag, *Local Quantum Physics* Springer, 2nd Edition, 1996.
47. I. J. R. Aitchison and A. J. G. Hey, *Gauge theories in Particle Physics*, Adam Hilger, Bristol and Philadelphia (1989), p.194.
48. G. Hoehler et al., Nucl. Phys. B **114** (1976), 505.
49. P. E. Bosted et al., Phys. Rev. Lett. **68** (1992), 3841.
50. S. Platchkov et al., Nucl. Phys. A **510** (1990), 740.
51. F. T. Hawes and M. A. Pichowsky, Phys. Rev. C **59** (1999), 1743.
52. J. C. R. Bloch *et al.*, e-print, nucl-th/9907120.
53. W. H. Press *et al.*, *Numerical Recipes*, Cambridge University Press, Cambridge, 1994.